MDC-G1174

NASA RADOME PROGRAM

September 1969

Prepared Under Contract NAS9-8865

by

Microwave Engineering Department
McDonnell Douglas Astronautics Company – Western Division
Santa Monica, California

for

NATIONAL AERONAUTICS AND SPACE ADMINISTRATION
MANNED SPACECRAFT CENTER
HOUSTON, TEXAS

MDC-G1174

NASA RADOME PROGRAM

September 1969

Prepared Under Contract NAS9-8865

by

Microwave Engineering Department
McDonnell Douglas Astronautics Company – Western Division
Santa Monica, California

for

NATIONAL AERONAUTICS AND SPACE ADMINISTRATION
MANNED SPACECRAFT CENTER
HOUSTON, TEXAS

CONTENTS

FIGURES

TABLES

Section 1
INTRODUCTION

This report covers the effort of McDonnell Douglas Astronautics Company (MDAC) in the design, development, manufacturing, testing, and installation of two broadband, multifrequency aircraft radiometer radomes for Manned Spacecraft Center, National Aeronautics and Space Administration (MSC, NASA). These radomes were required to perform at discrete frequencies in the L-, X-, K-, and K_a-bands, and in both vertical and horizontal polarizations. The transmission losses were to be minimal; pattern distortion and antenna beam deflection were to be within MIL-R-7705A (ASG), a military specification for radomes. Fitting of the radomes to the particular NASA P3A aircraft (927) was to be ensured. A determination was to be made of airworthiness for the chosen radome shape using aircraft operating parameters supplied by MSC.

Lightning arresters were to be installed that would not affect the radiation patterns, and temperature sensors were to be implanted in the radome which would give temperature readings with an accuracy of ±1/4° C.

Section 2
SUMMARY AND CONCLUSIONS

Two radomes that met the requirements were delivered to MSC. Contractually, verification of these radomes was to be made with simulated antennas and/or horns. At the request of the technical personnel of MSC, final patterns were made with the actual antenna system, antenna mounting ring, and simulated aircraft bulkhead structure, supplied as government furnished equipment (GFE) by MSC specifically for these tests. MDAC was thus able to furnish the government with measurements closely representing the system in its actual use configuration.

The original set of patterns taken on this system are being furnished to the government at no additional cost. These patterns are for four antenna look angles in the vertical plane (0°, 30°, 70°, and 160°); four frequencies (L-, X-, K-, K_a-bands); horizontal and vertical polarization; and for both radomes. Also furnished are corresponding patterns taken on the antennas only.

The final radomes were of solid laminate construction rather than the multiple sandwich. The two upper frequencies (K- and K_a-band) were almost precise multiples of the X-band frequency. Calculations showed that a laminate 0.265 in. thick produces electromagnetic transmission characteristics that meet the contractual requirements. An added advantage, in addition to the inherently stronger physical characteristics of this type of construction, is its ability to withstand the high-energy impact forces caused by hail. Hail impact tests made by Douglas Aircraft Company show that local delamination of the outer skin becomes negligible for aircraft in the P3A speed range when the skin is thicker than 0.080 in.

A hemispherical shaped radome was chosen to minimize any distortion of the antenna patterns. In general, the radomes performed within the tolerance of the military specification. In all cases boresight shift and beam spreading

were within the tolerance of the military specification. As far as side-lobe level changes in patterns, there were only two cases in which the change warrants explanation (see Subsection 6. 1).

The transmission efficiency tests performed by Jet Propulsion Laboratories showed that the losses caused by absorption generally were less than the contractual figure. Measurements made by MDAC were inconclusive, as was to be expected, since the measurement technique did not follow that called out in the military specification. Specified procedure requires that the radome be moved one-quarter of a wavelength with respect to the antennas. This could not be done with the GFE.

An aerodynamic analysis showed that the final radome shape did not have any adverse effect on the operational characteristic of the P3A aircraft. Also, its larger size did not restrict the vision of the pilots.

The larger size of this radome as compared to the usual P3A aircraft radome resulted in a somewhat heavier weight (approximately 280 lb). A stress analysis showed that existing latches, hinges, and former ring assembly could support this increase in weight.

The system required operation in both horizontal and vertical polarization. Therefore, solid lightning arrester strips were disregarded in favor of a technique developed by Douglas Aircraft Company which is insensitive to polarization. The manufacturing process of these arresters was improved by using photographic etching and plating procedures, giving significantly closer tolerances and uniformity of strips. Pattern tests were made with and without these strips on the radome and there was no appreciable change in the antenna patterns.

Section 3
DISCUSSION OF PROGRAM

3.1 MANAGEMENT

This program was managed in the MDAC Microwave Engineering and Laboratories Branch. The organization relationship shown in Figure 1 was established. John W. Thomas, Design Technology Director, held weekly or biweekly meetings depending on program needs and milestones. Full management support was given to ensure fulfillment of technical contract requirements and to meet the accelerated delivery schedule.

A decision was made in January 1969 that the contractor should be responsible for the actual fit of the radomes on the particular P3A aircraft. Measurements were made in Houston during January within 2 days after MDAC received the change of scope direction. The MDAC subcontractor, Fibco Plastics, made a master tool, molded to the configuration of the canted fuselage station to which the radome was attached.

To meet the accelerated schedule, two surplus radomes were purchased. The older radomes were removed and the former ring and associated hardware used for radome 1 on this contract. When the two sets of former rings furnished as GFE under Article XVII, Item 51, of the contract were received by MDAC, it was found that they were unusable for radome 2. Unfortunately, these rings were not drilled with pilot holes for the rivet hole pattern. As there are over 300 rivets closely spaced, the problem of drilling and backdrilling could have been formidable. It was decided, therefore, to use the ring from the second purchased radome in producing the second deliverable radome.

The first radome was completed on schedule and flown to Orlando, Florida at the request of MSC under a further change of scope. MDAC personnel accompanied the shipment. The radome 1 was fitted to the aircraft April 27 to the satisfaction of the MSC representative.

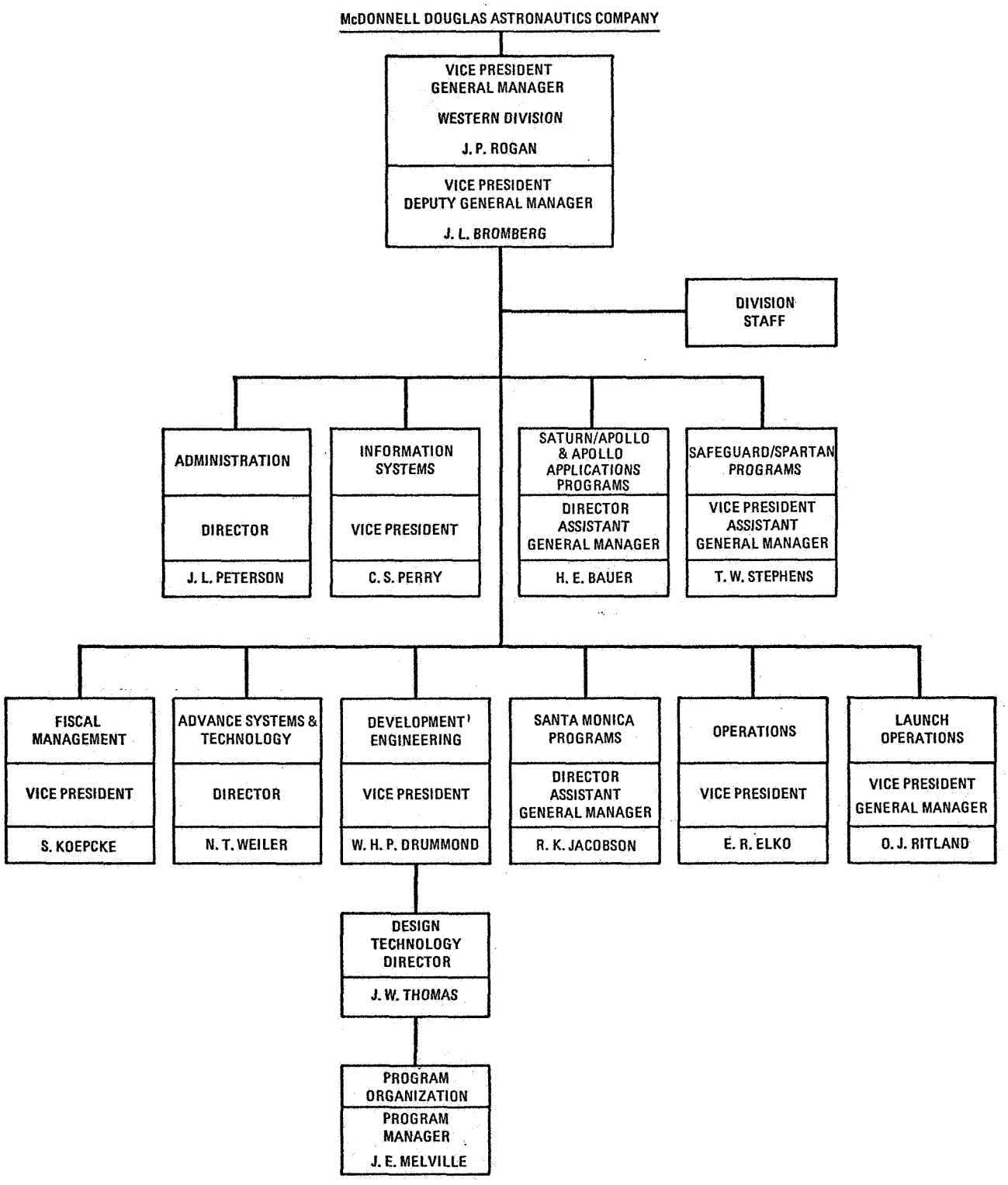

Figure 1. Program Organization

The second radome was completed early so that it could be fitted to the aircraft while the aircraft was in Houston for a checkup. This work was completed August 12.

3.2 SCHEDULE

MDAC responded to an August 1968 RFQ by a formal proposal in August 1968. A revised proposal was submitted in September 1968. In December 1968 a contract was received which allowed preliminary efforts to begin. In January, MDAC began full-scale development. In January, a change of scope was requested by MSC and in February MDAC made a formal proposal for added work against an accelerated schedule. The first radome was delivered in April and the second radome was delivered in August.

In July the antenna package, antenna mounting ring, bulkhead mockup section, and radome 1 became available. It was decided by MSC to supply this equipment as GFE to MDAC. Electrical tests were then run using the actual system and both radomes were measured within a week of each other. It had been planned to use reflectors and/or horns simulating the actual antenna system to verify the radomes. However, this change enabled MSC to get total system performance data plus preliminary patterns pending a more detailed measuring program. Data on the transmission efficiency phase of the measurements were made and calculations performed by Jet Propulsion Laboratories (to be released later as a JPL report).

3.3 DATA

There were 17 contractual data items required. Figure 2 shows the individual items and the dates completed.

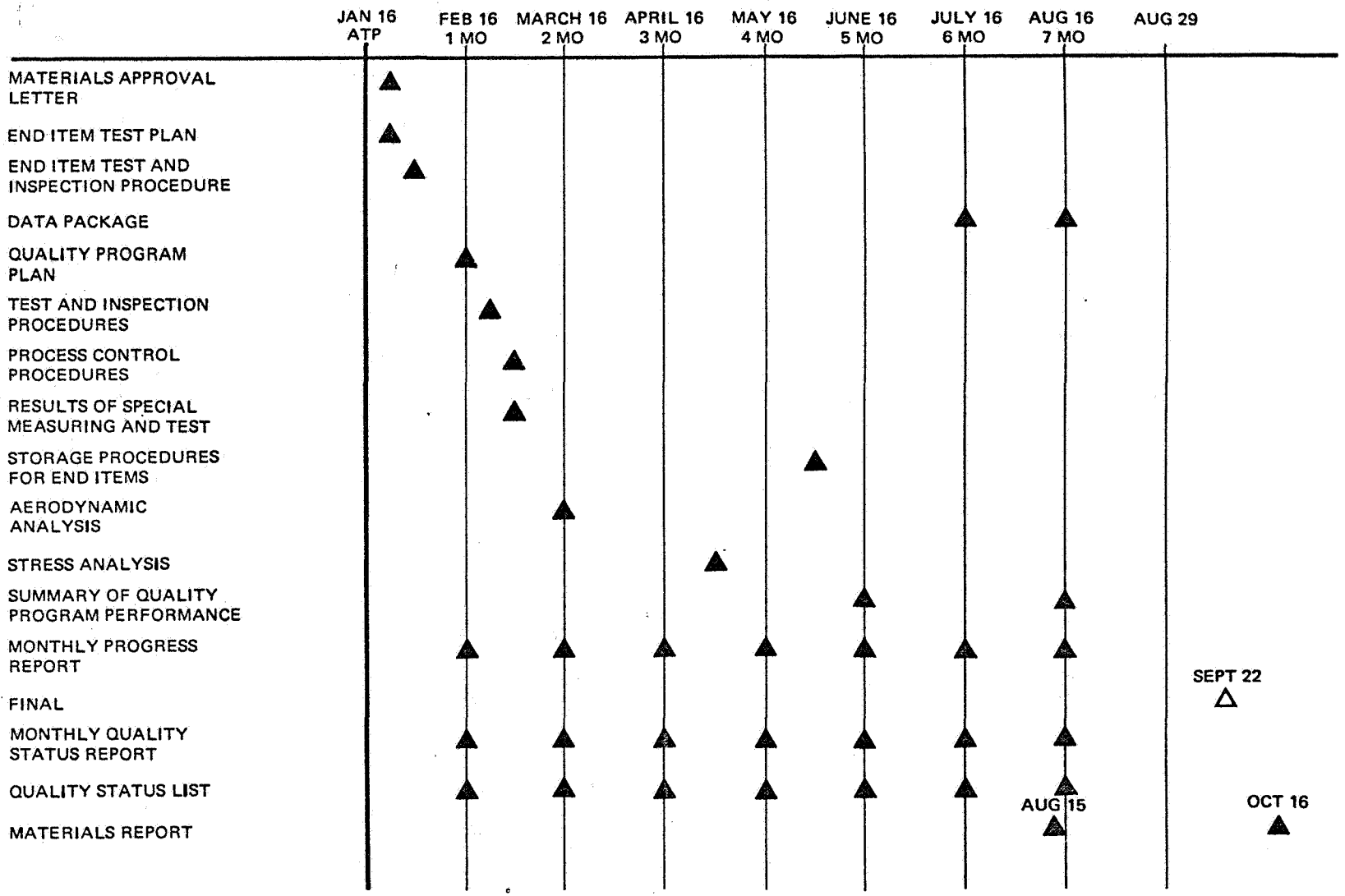

Figure 2. Contractual Data Items

Section 4

DESIGN

4.1 ELECTROMAGNETIC ANALYSIS

The radome made under this contract was unusual in that it was required to be transparent to a frequency spectrum greater than 20:1, whereas the majority of aircraft radomes are designed to pass a single specific frequency.

During analysis, the following steps were taken: (1) design studies, (2) selection of material, and (3) fabrication and test of a sample panel.

4.1.1 Design Studies

Radome design techniques may be generally divided into three categories. They are based on the three basic wall configurations: thin-wall, solid laminate, and sandwich.

The thin-wall radome has a wall thickness substantially less than one-tenth of the wavelength of the impinging energy. At relatively low microwave frequencies, such a wall is usually structurally adequate for most aircraft applications. However, at higher frequencies the thin-wall radome is normally not strong enough to withstand the flight conditions.

For maximum power transmission efficiency, the solid laminate should have a thickness of a half wavelength or some integral multiple thereof.

Several sandwich configurations are used. The simplest (A sandwich) consists of two very thin skins of relatively high dielectric constant, separated by a low-dielectric core whose thickness is an odd multiple of a quarter wavelength. Other sandwiches are the B type, where the core dielectric constant is higher than that of the skins; the C type, which has three skins and two cores; and the multilayer, which may have any reasonable number of layers of alternating high and low dielectric constant material. In the present design, all of these configurations were examined.

The first step in designing any radome is the grazing angle study. This procedure consists of locating the radiating system within the radome and examining the angles at which the radiated energy impinges on the radome wall. Knowledge of these angles is required because wall thickness is a function of incidence angle and relative polarization.

Figure 3 shows a profile view of the radome with accepted nomenclature and three positions of the antenna system. It will be noted that the incidence angle is that angle between the given ray and a normal to the surface at the point of impingement. The ray and the normal define the plane of polarization. When the electric vector is parallel to the plane, the polarization is defined as being parallel. Conversely, when the electric vector is perpendicular to that plane, the polarization is defined as perpendicular. In designing a radome, therefore, two conditions are examined: one where the electric vector (which defines the polarization) is oriented parallel to the plane of incidence; and the other, where the electric vector is perpendicular to the plane of incidence.

The basic step in selecting a wall configuration is a knowledge of the operational frequency of the system enclosed by the radome. In this case, a multifrequency radiometer system is involved. The frequencies of operation are:

1.42	±0.075 GHz	L-band
10.625	±0.125 GHz	X-band
22.3	±0.250 GHz	K-band
31.4	±0.250 GHz	K_a-band

An examination of the wavelengths shows immediately that a thin-wall radome would be structurally inadequate for a 400-knot airplane, since, even at the X-band frequency, it would be substantially less than 0.05 in. thick. Selection is thus constrained to either the solid wall or the sandwich.

Examining the simplest sandwich, it is seen that the frequencies are so related that a quarter-wave core at 10.625 GHz would be a half-wave core at 22.3. This constitutes the poorest possible sandwich, thus eliminating such a configuration from consideration.

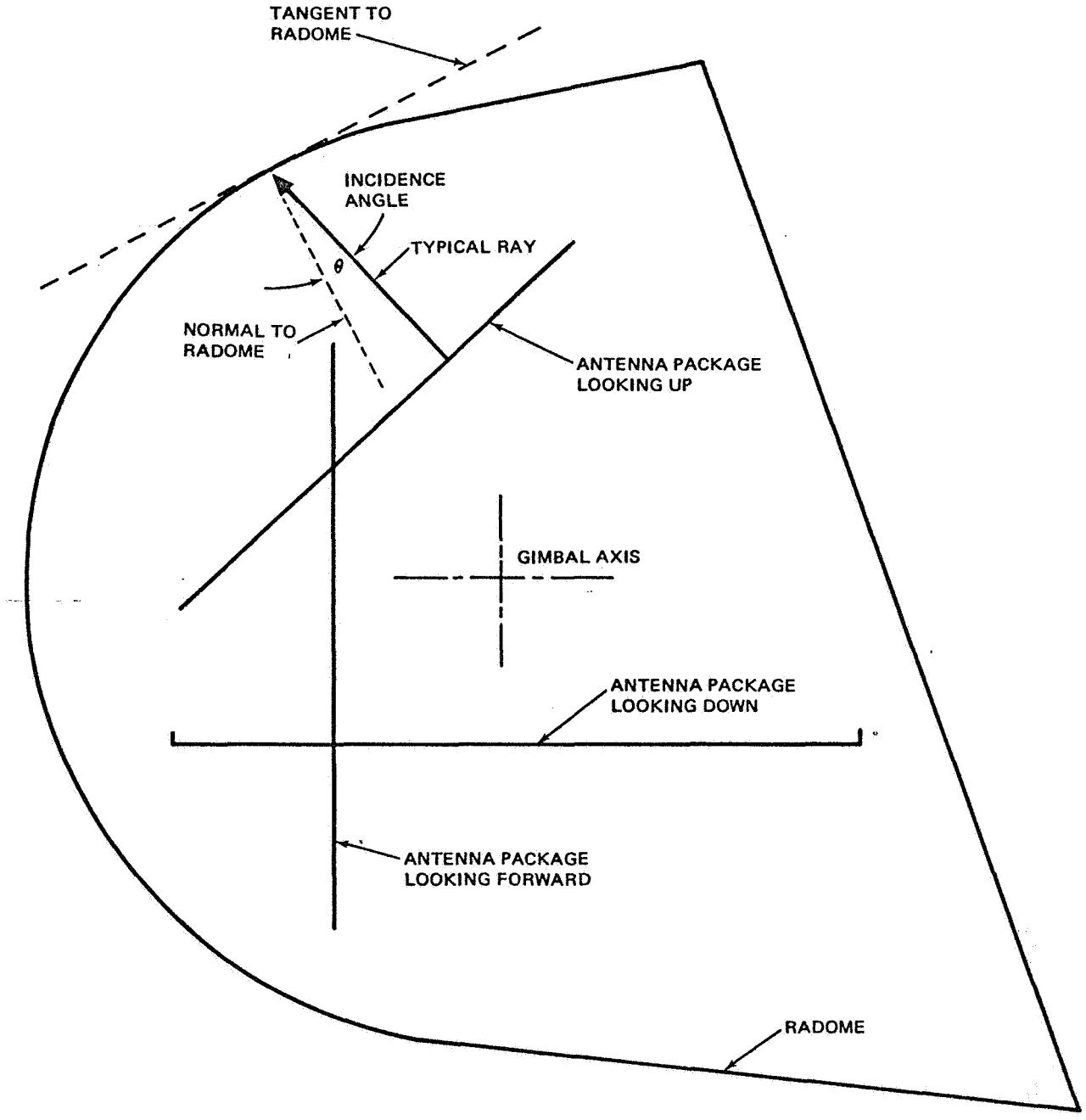

Figure 3. Radome-Antenna Nomenclature

In the case of the B-sandwich, two factors mitigate against its practicality for the present application. First, the dielectric constant required for the core is unreasonably high. Secondly, since the skin thickness must be a quarter wavelength, the multiplicity of frequencies makes selection of a skin dimension impractical. This is the identical problem which arises with the core of the A-sandwich.

Multilayer sandwiches are based upon a number of very thin (0.010 to 0.020 in.) skins, separated by lightweight cores, each about 0.100 in. or less. The requirement in this radome for resistance to rain erosion and to hail impact implies an outer skin at least 0.040 in. thick, plus about 0.012-in. neoprene or urethane protective coating. Such an outer skin would actually mitigate strongly against selection of the multilayer wall.

Thus the thin wall and the sandwich are eliminated, leaving the solid laminate. Normally, because of the half-wave consideration, this configuration cannot be considered broadband. However, the three upper frequencies bear almost a precise harmonic relationship. Thus, a half-wave wall at X-band becomes a full-wave wall at K-band and three-halves wave wall at K_a-band. At the lowest frequency, such a wall approaches the thin-wall criteria.

Power illumination contours were assumed for the four system antennas, based upon the known characteristics of arrays and of scalar horns. Figure 4 shows the distribution of energy across the face of the aperture in the X-, K-, and K_a-band scalar horns. The assumed distribution conforms to the cosine curve, with no energy at the outer edge. Similarly Figure 5 shows the assumed distribution as taken from the literature, for the L-band array. The level at the aperture edge is -20 dB. Using these contours and the conventional grazing angle procedure, it was determined that, in the almost hemispherically shaped radome, the weighted average incidence angles for the four antennas are shown in Table 1. As would be expected from a hemispherical shape, the incidence angles are very low.

Based upon a measured dielectric constant of 4.28 and loss tangent of 0.014 for a conventional glass-epoxy laminate, a study was made by electronic computer to find the power transmission efficiency, power reflection, and insertion phase delay of the solid wall as functions of frequency, incidence

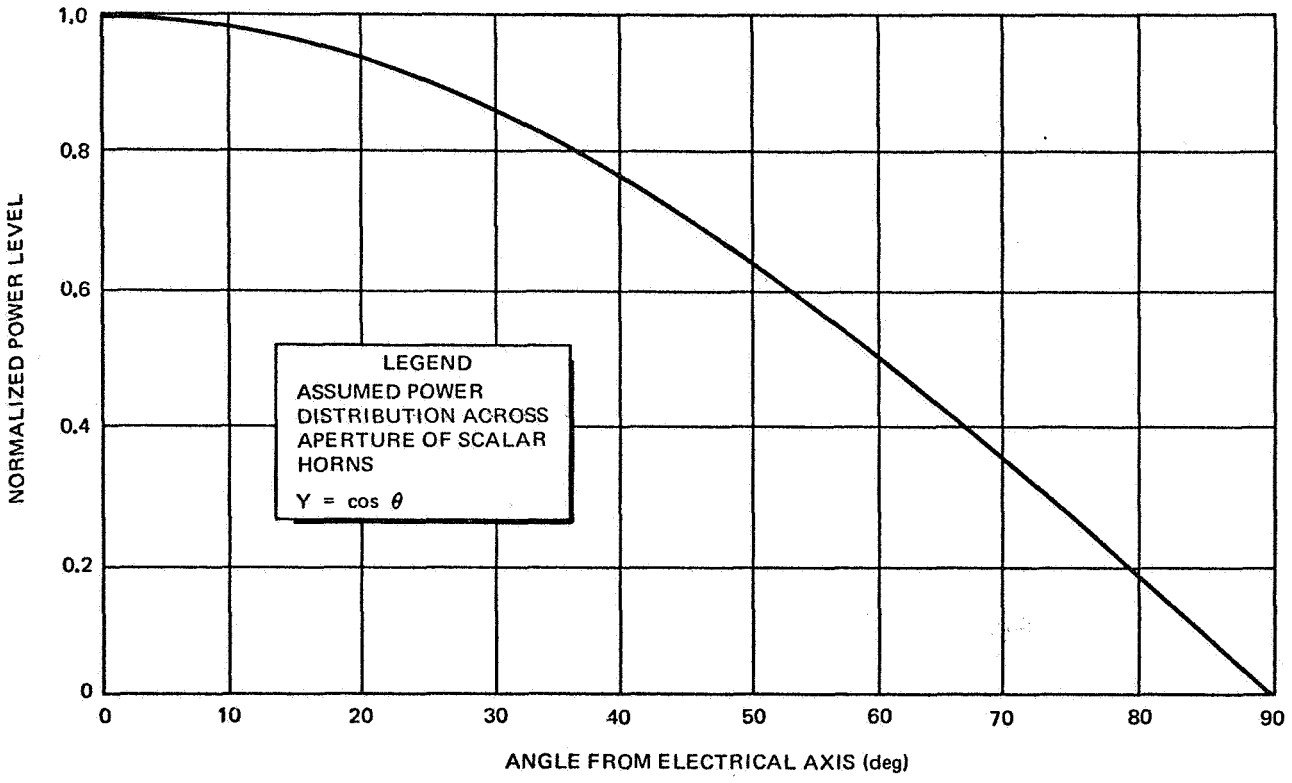

Figure 4. Near-Field Antenna Illumination Pattern – Scalar Horns

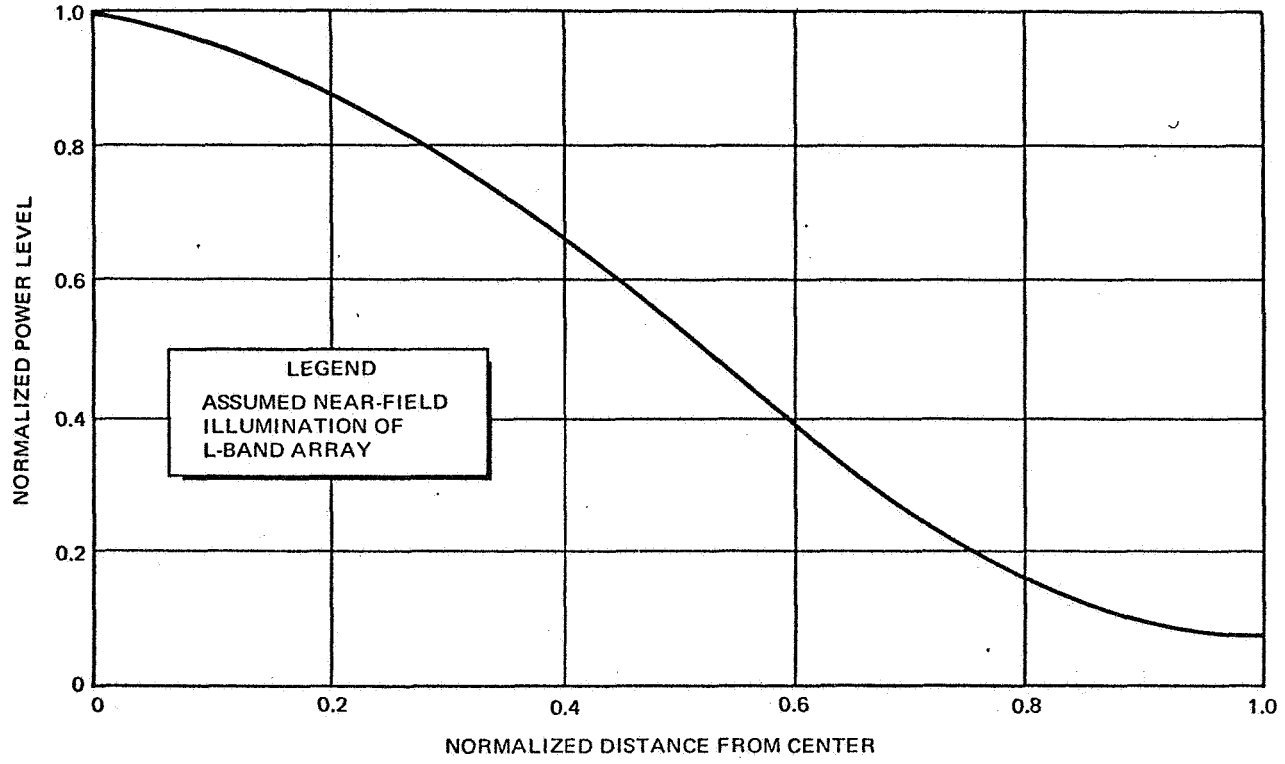

Figure 5. Near-Field Antenna Illumination Pattern – Phased Array

Table 1

WEIGHTED AVERAGE INCIDENCE ANGLES

Frequency	Aspect		
	Forward	Up	Down
L-band	10°	8.25°	10.4°
X-band	12.5°	13.0°	3.3°
K- and K_a-band	14.3°	14.4°	10.4°

angle, and polarization. Curves were plotted to show the results of these calculations. Individual sets were first laid out for each discrete frequency band. A composite set was then drawn to show the overall response of the radome at all primary frequencies. These curves are also shown in Figures 6 through 10.

4.1.2 Selection of Material

Eight sample laminates were submitted by the subcontractor, Fibco Plastics. Dielectric measurements were made and the results are shown in Table 2. The configuration selected was laminate 5. The radome wall was constructed with two layers of type 181 glass cloth (0.0085 in. thick) as inside and outside surfaces. Between these layers, the remaining laminate was of type 1584 glass cloth (0.026 in. thick). The resin selected for impregnation was Shell epoxy, type 828, using curing agent A. This laminate had a resin content of 28%, resulting in a dielectric constant of approximately 4.1 and a loss tangent of 0.01. The thickness was 0.265 in.

4.1.3 Fabrication and Test of Sample Panel

A 2 by 4 ft test panel was then fabricated using the above configuration. It was tested in accordance with the procedure in paragraph 4.8.3.2.2 of MIL-R-7705A (ASG). The results are tabulated in Table 3.

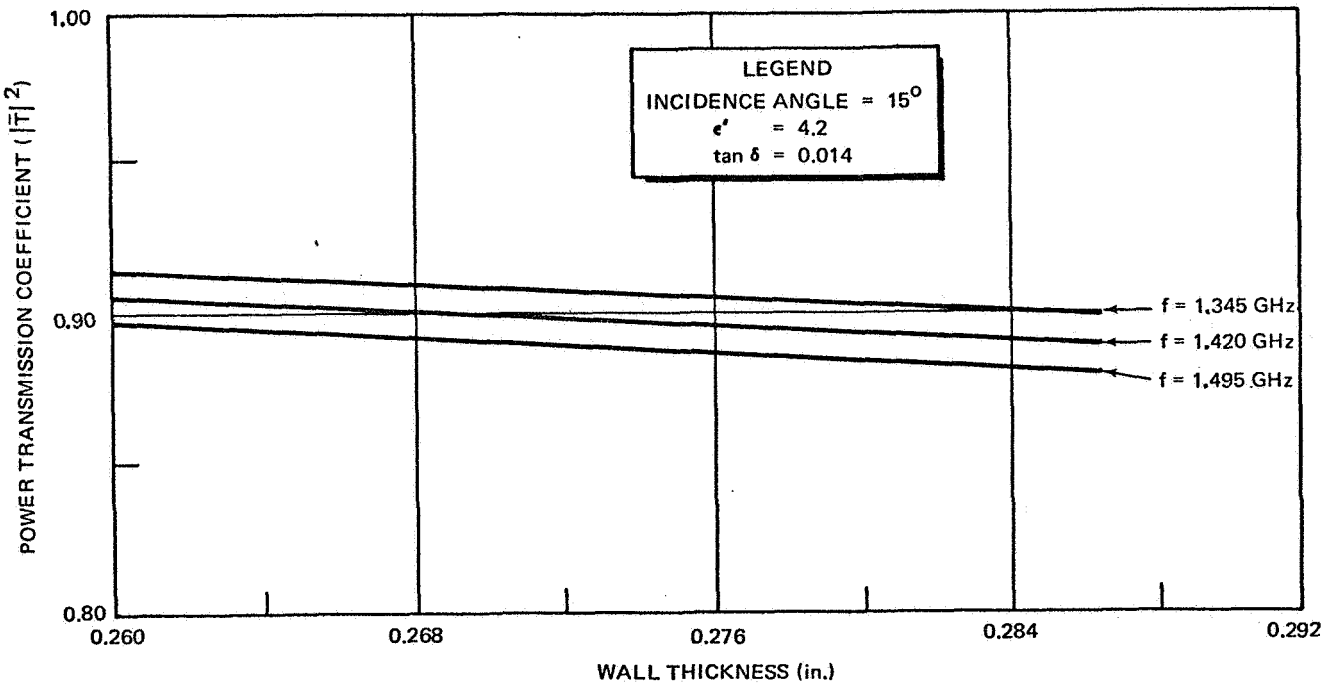

Figure 6. Efficiency of Solid-Wall Radome at L-Band

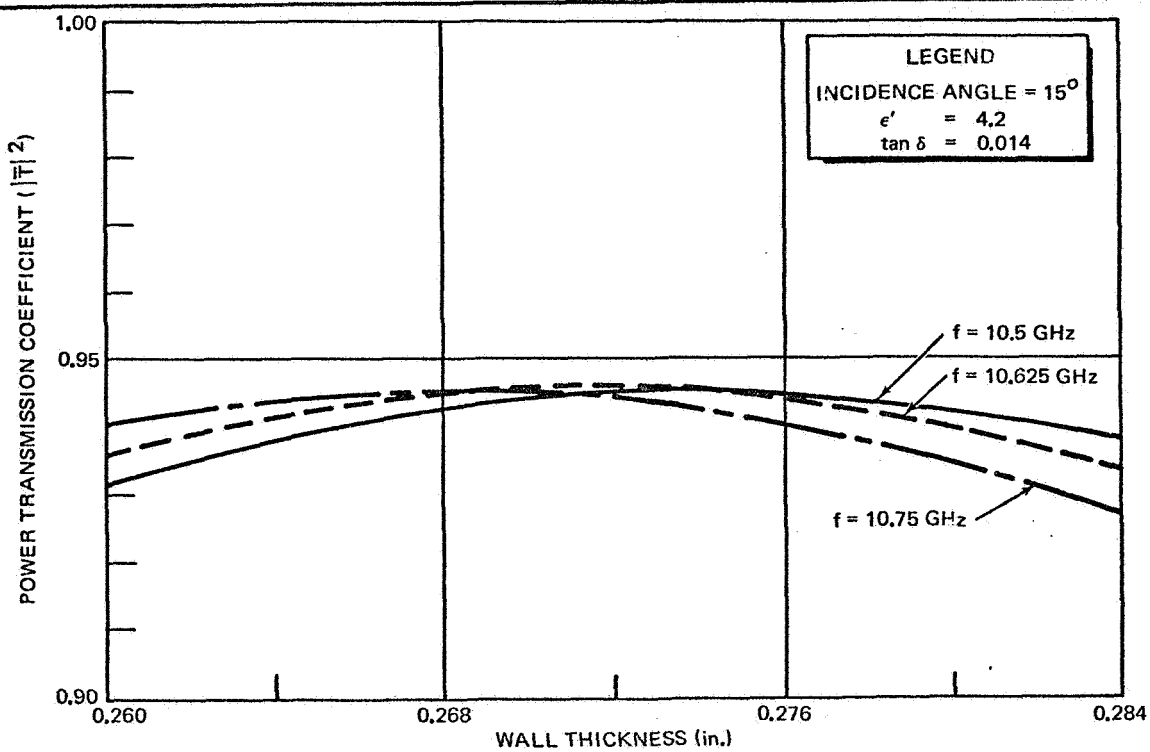

Figure 7. Efficiency of Solid-Wall Radome at X-Band

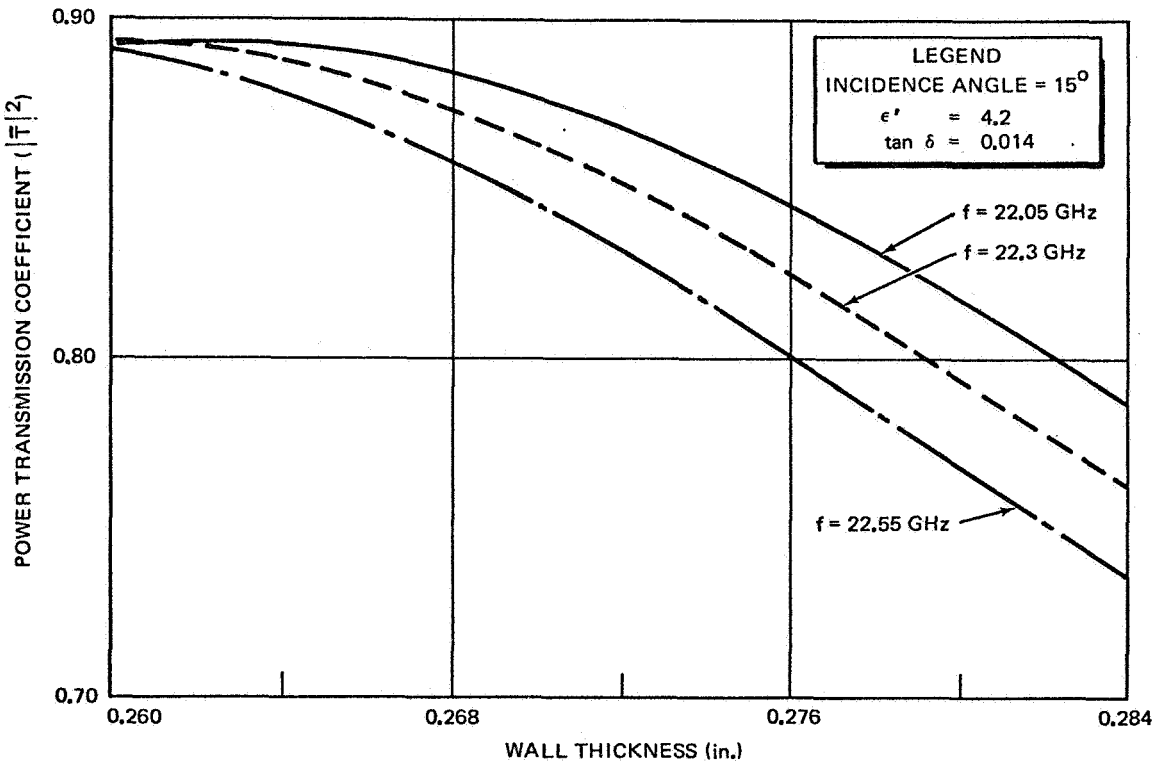

Figure 8. Efficiency of Solid-Wall Radome at K-Band

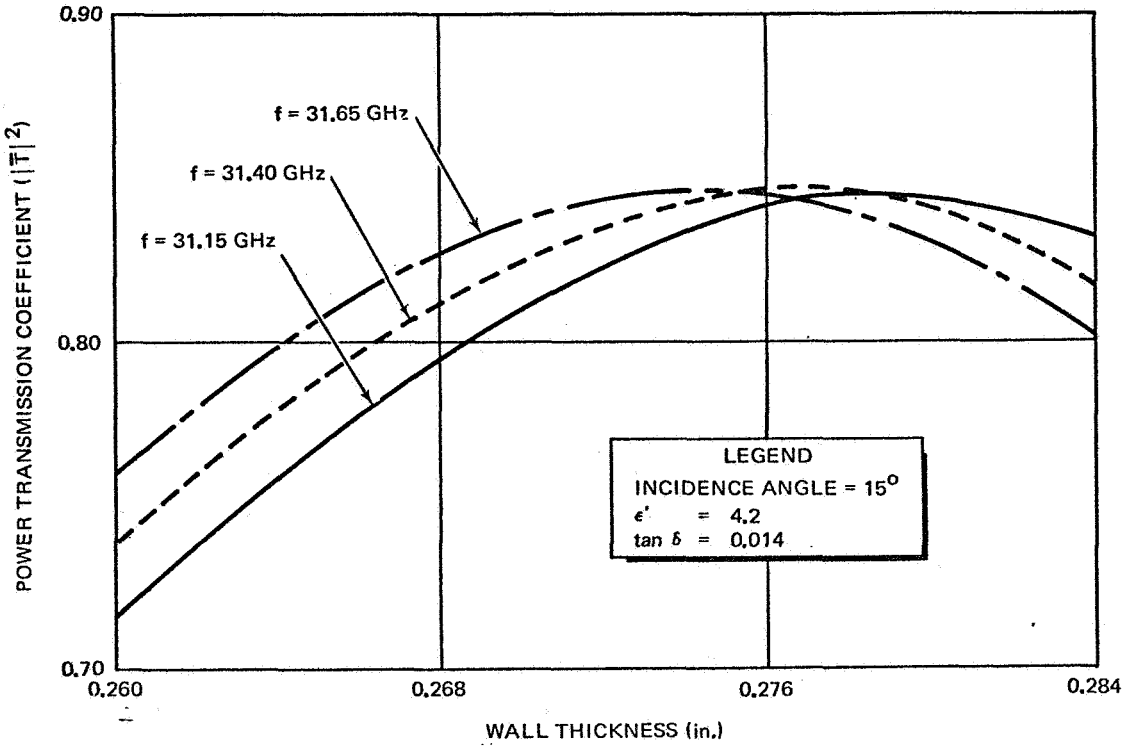

Figure 9. Efficiency of Solid-Wall Radome at K_a-Band

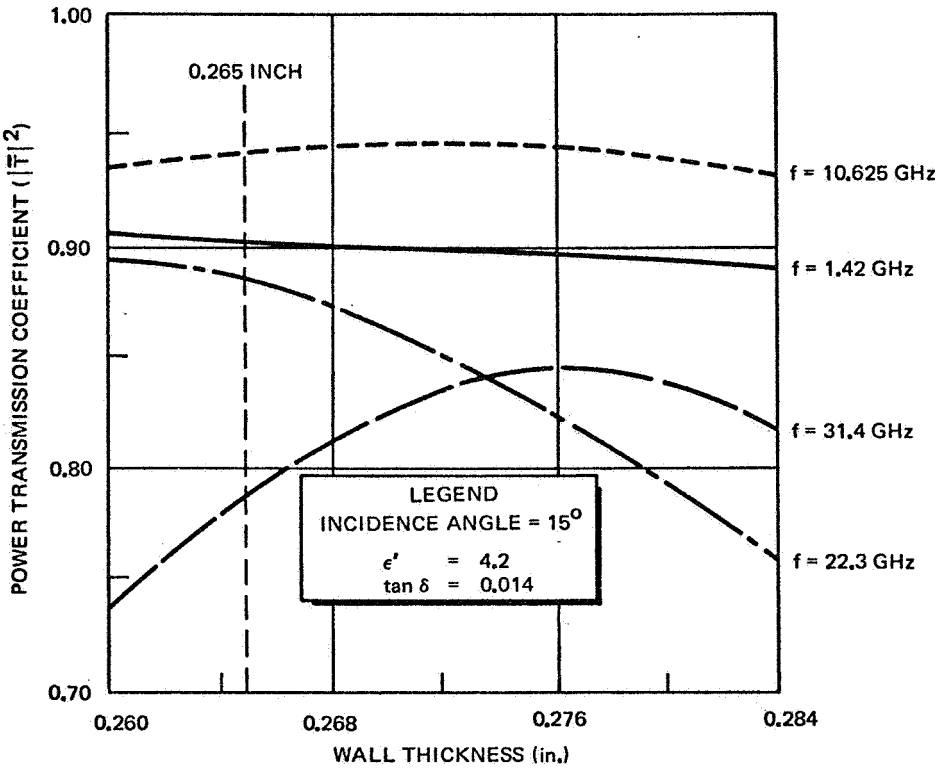

Figure 10. Composite Performance of Solid-Wall Radome

4.2 AERODYNAMIC ANALYSIS

MDAC was to perform an aerodynamic analysis to determine the aerodynamic loads on the radome shell and the attachment fittings. Also there was to be an estimate of the resulting aircraft and flight restrictions, if any.

This phase of the contract was performed by personnel in the Douglas Aircraft Company because of their extensive experience in this type of analysis.

An estimated pressure distribution over the forward 100 in. of the fuselage of the P3A was made. The calculations were based on Douglas three-dimensional Neuman computer program, BOXC.

A comparison between the profiles of the existing and the new radome in both vertical and horizontal planes showed a very small increase in planform and side area of the fuselage. This increase in area and fuselage volume is not large enough to have significant effect on either the longitudinal or directional stability or controllability of the aircraft.

Table 2

DIELECTRIC SAMPLE MEASUREMENTS

Laminate No.	Glass Type	Resin Type	Resin (Percent)	Dielectric Constant	Loss Tangent
1	1584	DiCo Polyester 6622	28	4.23	0.0054
2	1581	DiCo Polyester 6622	28	4.06	0.005
3	1581	Shell Epoxy 828 APCO 180 Hardener	28	4.47	0.027
4	1581	Shell Epoxy 828 Curing Agent A	28	4.11	0.017
5	1584	Shell Epoxy 828 Curing Agent A	28	4.14	0.010
6	1584	Shell Epoxy 828 CL Hardener	32.4	3.89	0.013
7	1584	Shell Epoxy 828 CL Hardener	32.4	4.08	0.024
8	1584	Shell Epoxy 828 CL Hardener	32.4	4.05	0.024

Table 3

FLAT-PANEL TEST RESULTS

θ(Deg)	Frequency (GHz)					
	10.8		22.3		31.4	
	Perpendicular Polarization (%)	Parallel Polarization (%)	Perpendicular Polarization (%)	Parallel Polarization (%)	Perpendicular Polarization (%)	Parallel Polarization (%)
0	90	90	81	81	76	76
5	92.5	90	85	80	74	85
10	91.5	90	81	80.5	72.5	89
15	91.5	91.5	83	85	72.5	84
20	90	90	83	83	74	84
25	90	91.5	82	84	72.5	86.5
30	89	92.5	82	85	70	85.5
35	88.5	91.5	81	85	69	85.5
40	87	91.5	81	86	62	84
45	84	91.5	79	85	60	84

Therefore, no restrictions were imposed on the normal operating envelope and center-of-gravity range of the P3A aircraft.

The results of this analysis have been given in report DAC-67784, a copy of which has been supplied as Data Item 11.

4.3 STRESS ANALYSIS

The original RFP required that the radome be capable of withstanding the takeoff, flight, and landing stress conditions. The interface for responsibility between MDAC and MSC was that MDAC would make an analysis of structural loads to the hinges and latches due to the radome, but would not consider the transfer of stress into the aircraft structure. This phase of the contract was also performed by personnel in the Douglas Aircraft Company.

Because of the lack of pertinent data on the P3A aircraft, it was agreed among MSC, MDAC, and Douglas Aircraft Company personnel that Douglas Aircraft would develop the appropriate information from C-133 basic flight data. Originally these data were to be supplied as GFE, Item 48 Article XVII of the Contract. Subsequently, Douglas Aircraft developed an Aircraft Lift Coefficient versus Angle of Attack versus Mach Number criterion. In addition, a Pitch Attitude Envelope was developed. Four aircraft were used to determine an average value of angle of zero lift to use for the P3A. The four aircraft were the C-133, C-124, DC-6, and DC-8.

An equivalent airspeed of 405 knots was chosen as the maximum velocity for the P3A by MSC.

Computer program SA-39 was used to calculate internal loads and moments for an external pressure distribution on the radome. Margins of safety were calculated for the radome, hinge assembly, latches, and former assembly.

The results of these analyses are given in an extensive report DAC 67785, a copy of which has been supplied as Data Item 12.

4.4 LIGHTNING ARRESTERS

The Douglas Aircraft Company has had extensive experience with the configuration of lightning arresters on such proven aircraft as the DC-6, DC-7, DC-8, and DC-9 airplanes. This experience was the basis for the lay-out of the arresters on these radomes (see Figure 11). Solid-conductor strips were used on these aircraft because the radars enclosed in the radomes were of one polarization. The dual polarization imposed on the radome design for this contract made it advisable to proceed directly to a Company-developed technique which minimizes antenna pattern distortion caused by the arrester. The accelerated schedule reinforced this decision. Details are shown in Figure 12.

Printed circuit techniques are used that permit accurate scaling and allow large quantity production. A high resistive film is coated along the back of the arrester and gives a continuous path to the lightning discharge. Should the radome receive a direct lightning strike, the electrical path is initially set up across the square dots and the carefully controlled air gap (0.020 ± 0.001 in.). The main current flow subsequently takes place through the ionized path above the arrester.

Epoxy adhesive is used to apply the strip to the radome. A specifically designed paddle section is used to connect the end of the arrester to the former assembly.

4.5 TEMPERATURE INDICATORS

Seven temperature sensors were located around each radome according to Figure 13. These sensors were placed on the outside of the radome top, bottom and side, on the inside of the radome top, bottom and side, and one embedded in the radome on the side. The accuracy specified by the contract (-55°C to 45°C within ±1/2°C and -30°C to 25°C within ±1/4°C) made it necessary to put the seven amplifiers in two temperature-controlled ovens. Figure 14 shows the wiring diagram. The ovens were purchased from Thermal Systems, Incorporated and are shown in Figure 15.

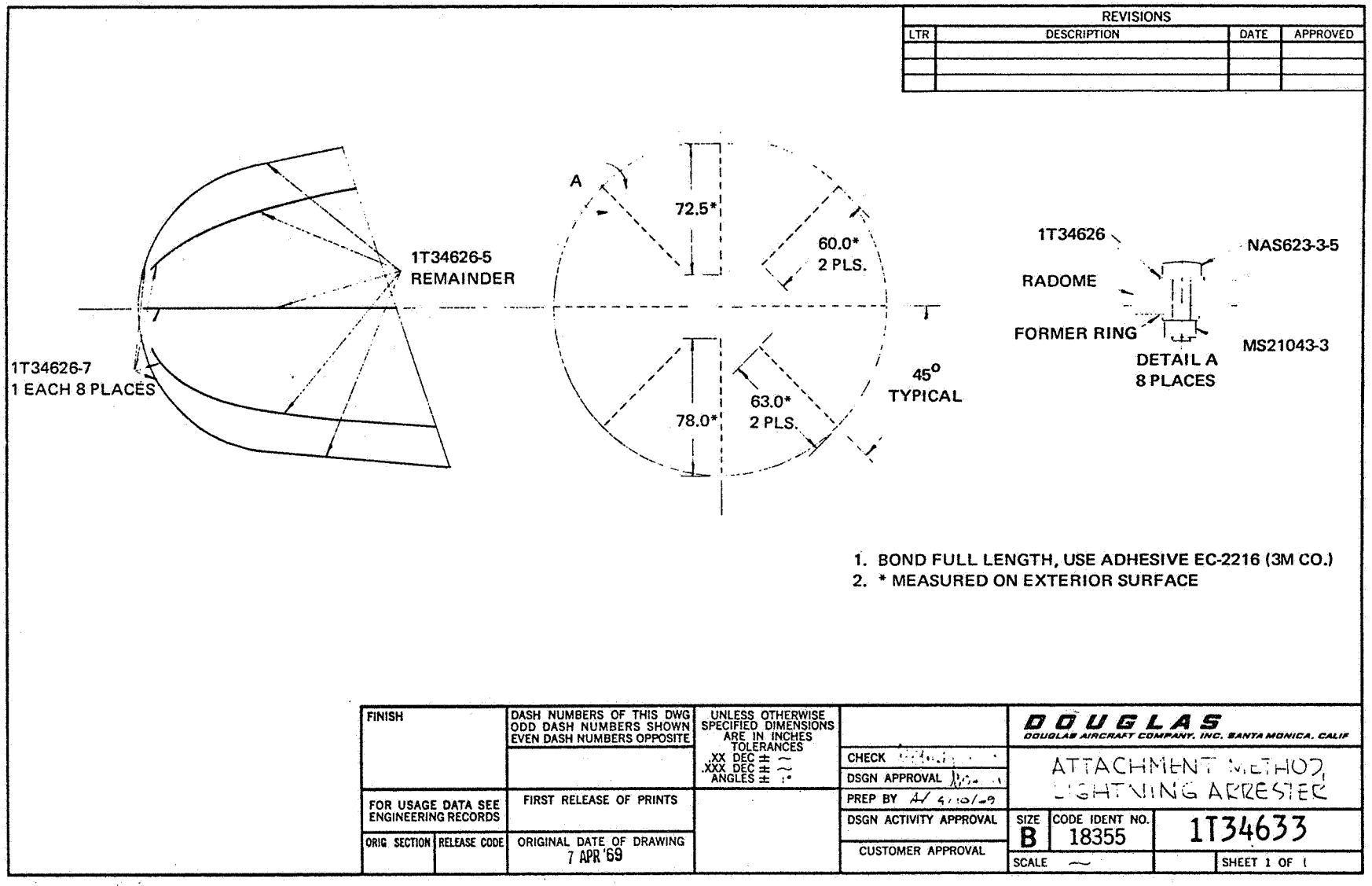

Figure 11. Attachment Method – Lightning Arrester

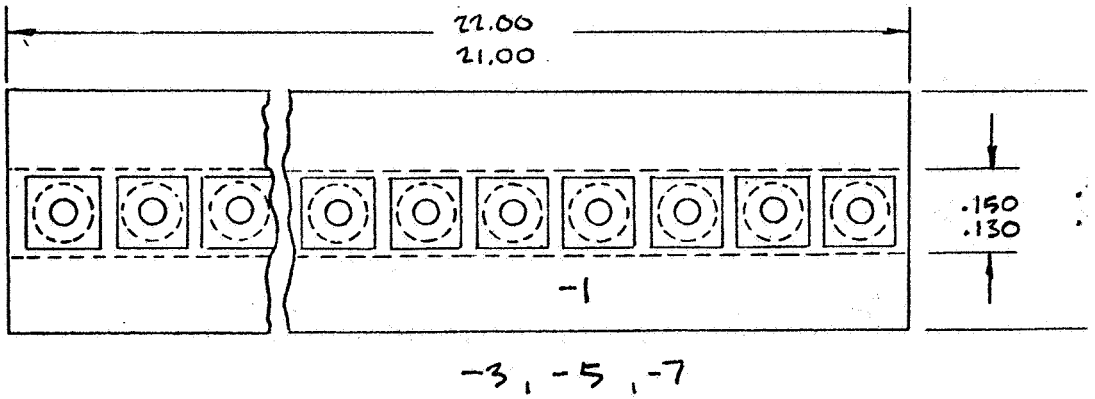

-3, -5, -7

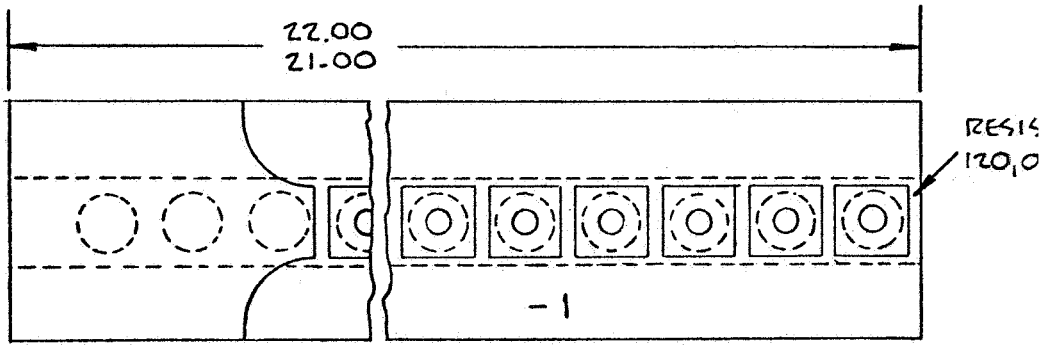

-501

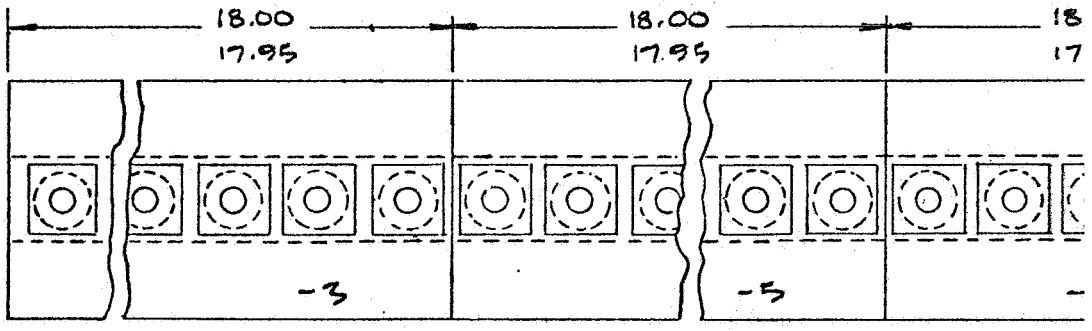

-503

FINISH		DASH NUMBERS ODD DASH NU EVEN DASH NUM
FOR USAGE DATA SEE ENGINEERING RECORDS		FIRST RELEAS MAR 2
ORIG SECTION	RELEASE CODE	ORIGINAL DAT 25 M

REVISIONS			
LTR	DESCRIPTION	DATE	APPROVED
A	ADD NOTES, RES. COAT DES. -3, -5-7, ADD ALT. MAT'L.	4/1/69	S.S. Oleesky

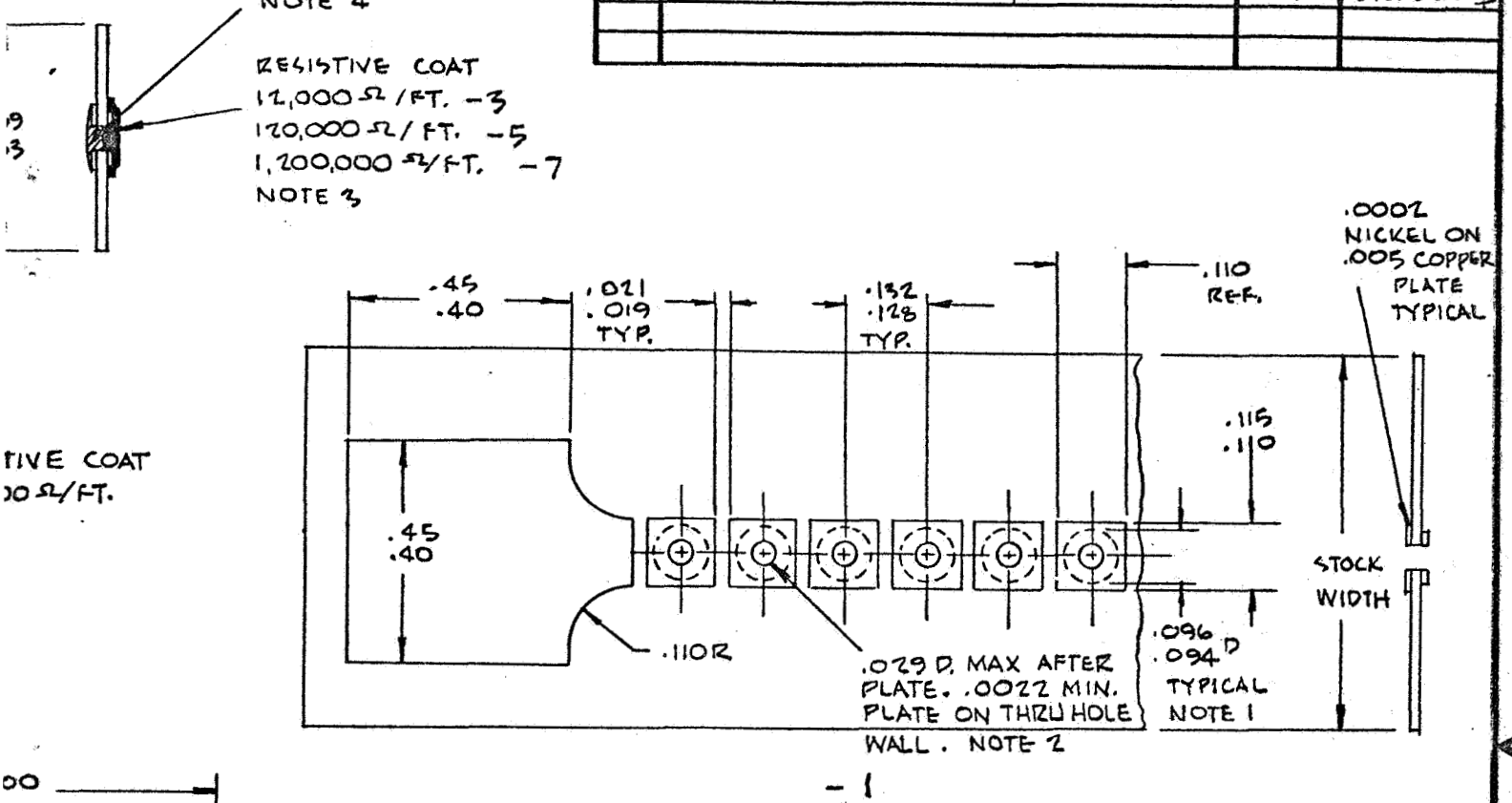

GENERAL NOTES:

1. REGISTRATION OF TOP & BOTTOM ETCHED PLATING CENTERS WITHIN A CIRCLE OF .005 DIAMETER.
2. REGISTRATION OF ETCHED PLATING & DRILLED HOLES' CENTERS WITHIN A CIRCLE OF .010 DIAMETER
3. REGISTRATION OF RESISTIVE COAT & ETCHED PLATING CENTER LINES WITHIN A STRIP ZONE OF .032 WIDTH.
4. WAVE SOLDER 60/40 FROM SQUARE BUTTON SIDE.

OF THIS DWG BERS SHOWN BERS OPPOSITE	UNLESS OTHERWISE SPECIFIED DIMENSIONS ARE IN INCHES TOLERANCES .XX DEC ± ~ .XXX DEC ± ~ ANGLES ± ~	CHECK James S. Brooks	DOUGLAS AIRCRAFT COMPANY, INC. SANTA MONICA, CALIF
		DSGN APPROVAL Wayne Lewis	LIGHTNING ARRESTER
E OF PRINTS 1969	MATERIAL CORE LAMINATE STM0054-010504 OR STM0054-010507	PREP BY AJ 3/25/69	
OF DRAWING R '69		DSGN ACTIVITY APPROVAL	SIZE B / CODE IDENT NO. 18355 / 1T34626
		CUSTOMER APPROVAL	SCALE 4 : 1 / SHEET 1 OF 1

Figure 12. Lightning Arrester

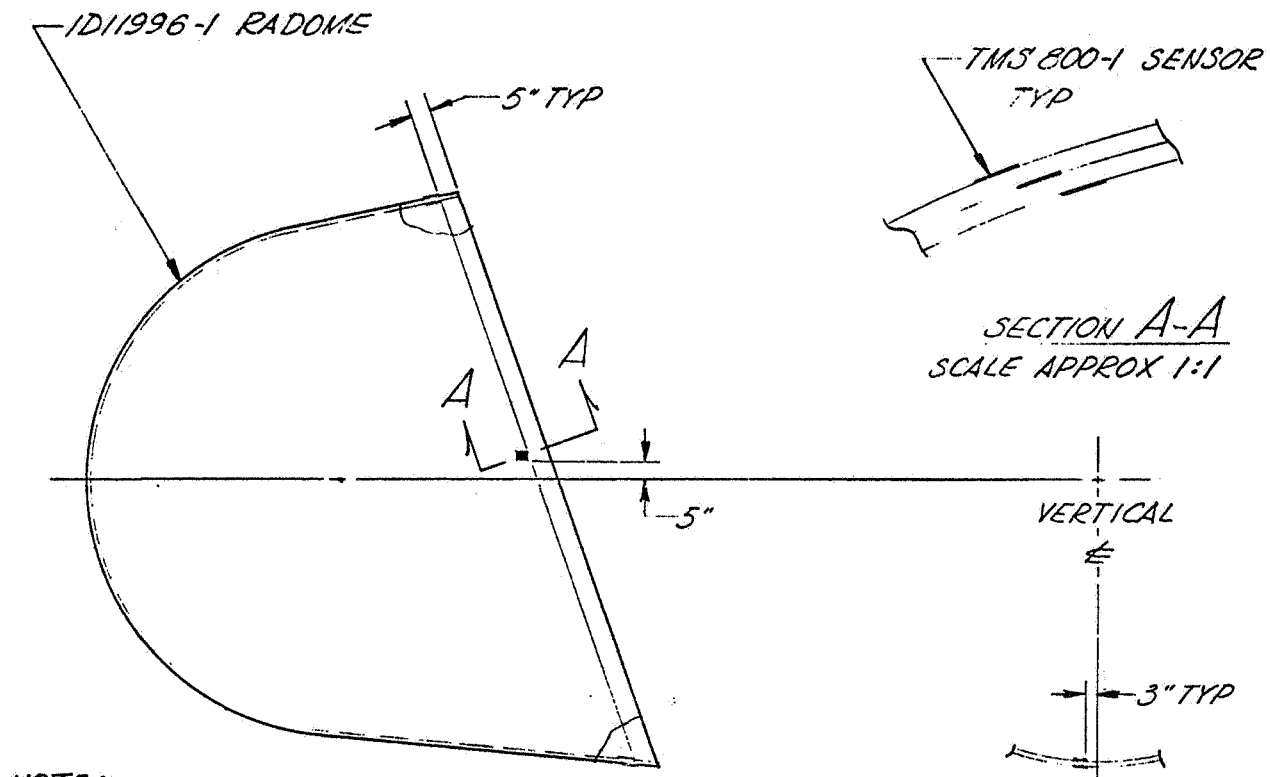

NOTE:

1. BRIDGE MOUNTING BRACKETS TO BE WITHIN 9" OF SENSORS.
2. WIRE PER IT35253 SCHEMATIC.
3. TMS 800-1 SENSORS INSTALLED APPROXIMATELY AS SHOWN.
4. HOLES FOR SENSOR LEADS TO BE DRILLED AS REQUIRED & FILLED WITH EPOXY RESIN.
5. SC 630-1 AMPLIFIERS TO BE INSTALLED ON SUPPORT ROD BRACKETS LOCATED ON HORIZONTAL CENTERLINE, 2 PLACES.

Figure 13. Temperature Sensor Location

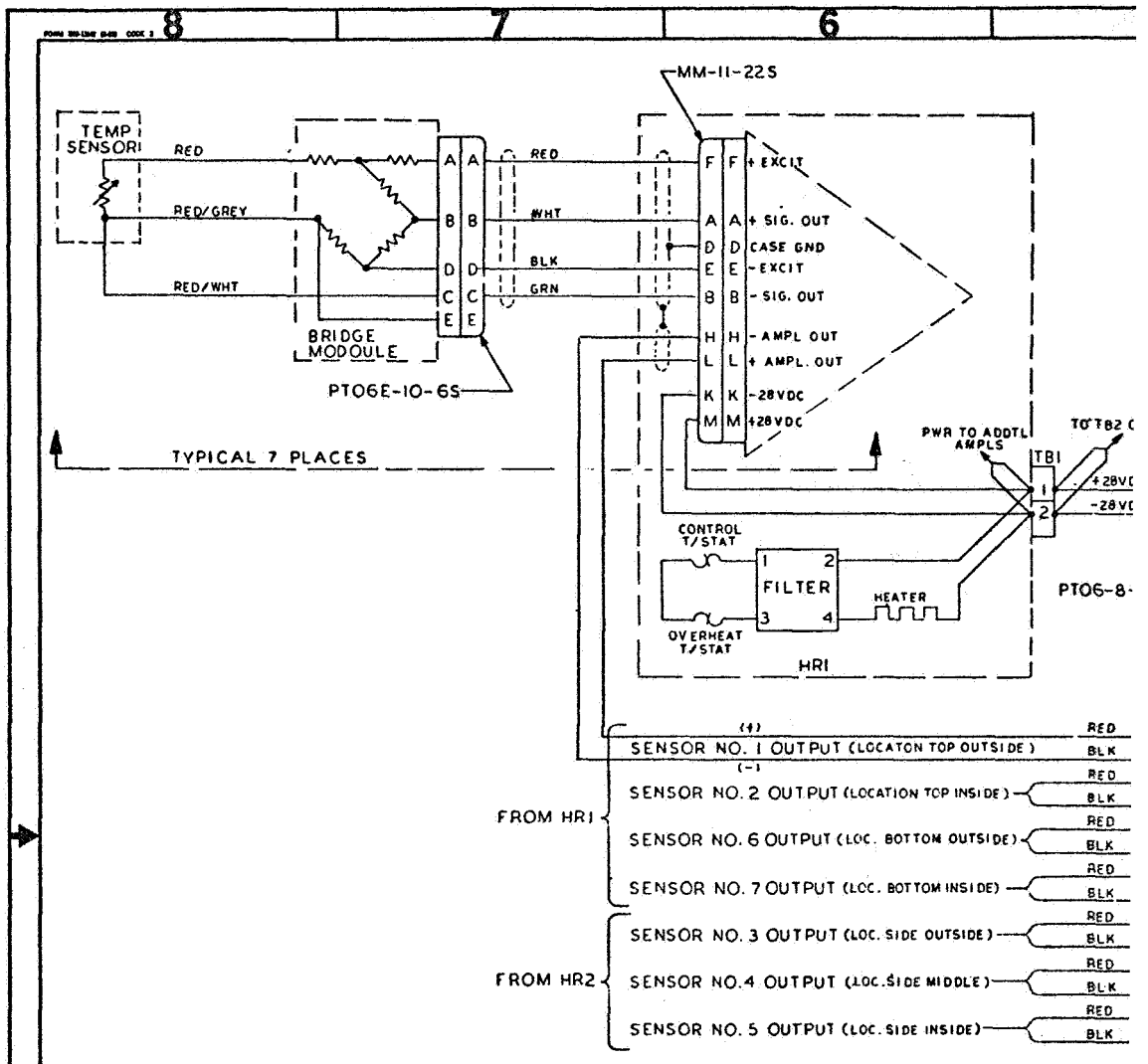

REF. DES	PART NUMBER	PART DESCRIPTION
TB1 TB2		TERMINAL BLOCK FURNISHED AS PART OF HR1 AND HR2 OVENS
P15	PT06-8-3P	BENDIX
P8 THRU P14	MM11-22S	CONTINENTAL
P1 THRU P7	PT06E-10-6S	BENDIX
P16	PT06-2C-27S	BENDIX
HR1 HR2	21-2789	OVEN THERMAL SYSTEM INC
AMPL SN.001 TO SN.010	SC630-1	INSTRUMENTATION AMPLIFIER TYLAN CORP
SENSOR NO.1 THRU NO. 7	TMS8C0-1	PLATINUM TEMP SENSORS TYLAN CORP

REFERENCE DESIGNATION LIST

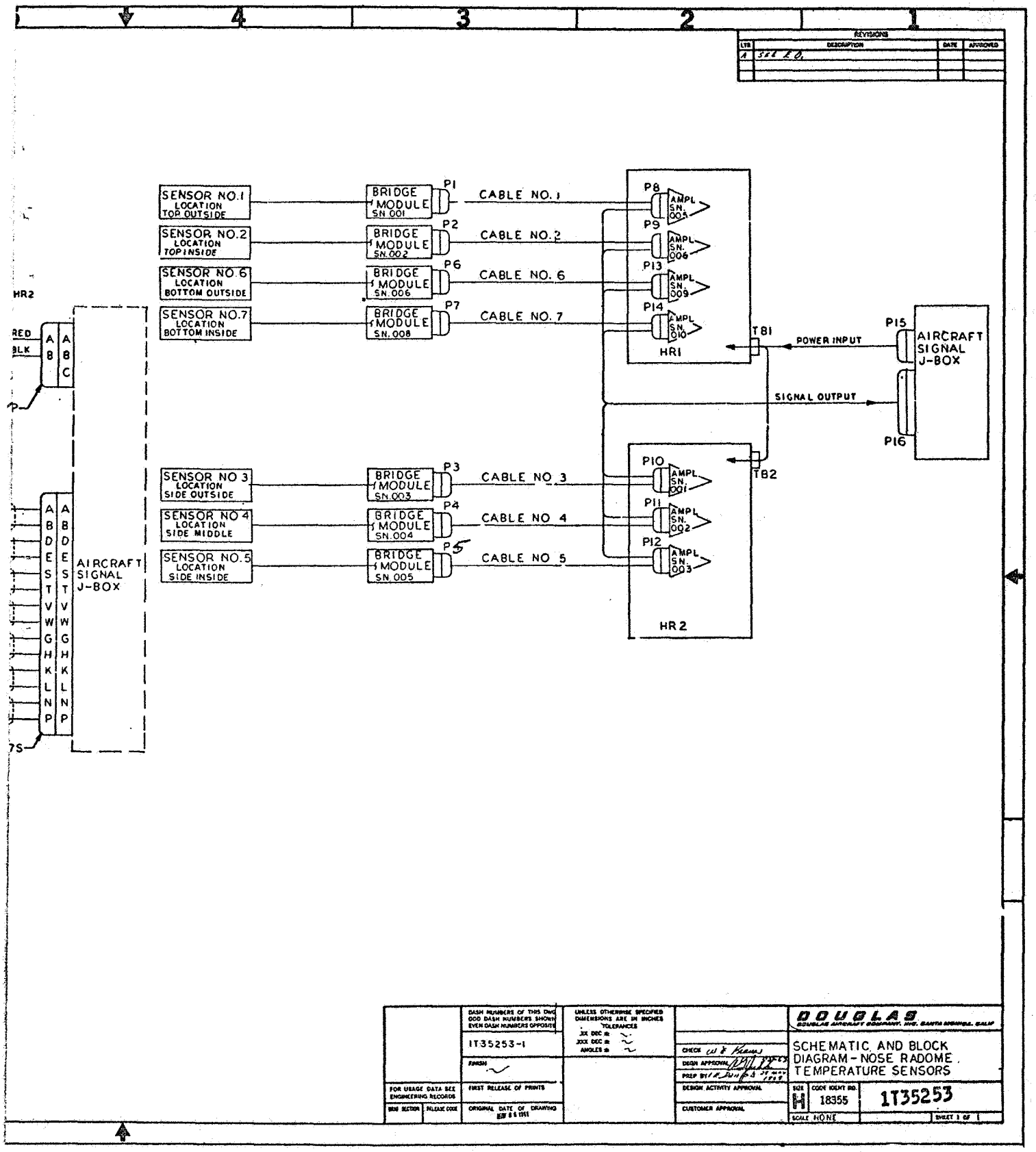

Figure 14. Temperature Sensor Wiring Diagram

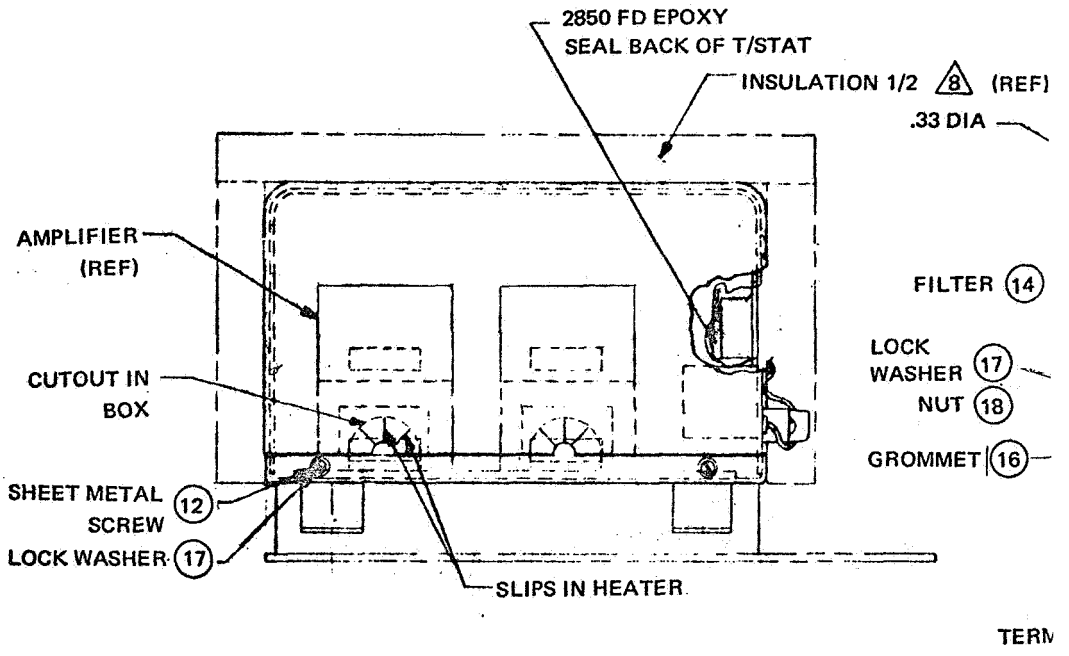

Figure 15. Temperature Sensor Oven

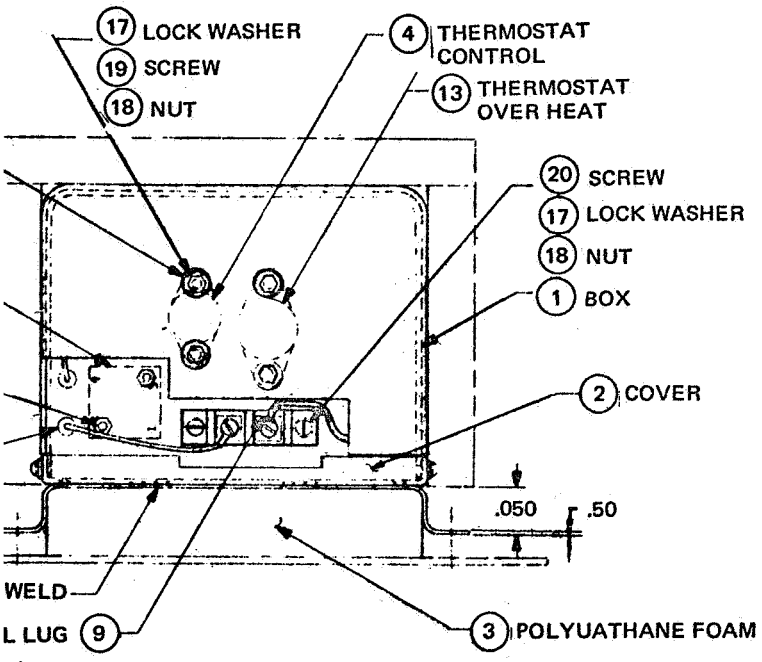

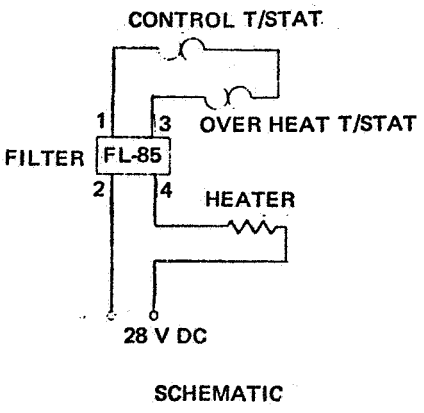

SCHEMATIC

NOTES:

1. HEATER SHALL OPERATE AT 28 V DC & WATTAGE SHALL BE 40 + 10%
2. RESISTANCE OF HEATER SHALL BE MIN & MAX
3. CONSTRUCTION SHALL BE LAMINATES OF SILICONE RUBBER IMPREGNATED FIBERGLASS ENCASING NICKEL CHROMIUM RESISTANCE WIRE
4. OPERATING TEMPERATURE OF HEATER SHALL BE
5. CONTROL THERMOSTAT TO OPEN AT 75 $\pm$ 5°F & CLOSE AT 45 $\pm$ 5°F.
6. MARKED APPROX. WHERE SHOWN:
   MFG. THERMAL SYSTEMS INC.
   P/N 21-2789
   VOLTS 28 DC, WATTS
7. OVER HEAT THERMOSTAT TO OPEN AT 102 = 5°F & CLOSE AT 50 50 $\pm$ 5°F.
8. INSULATION COVER SHALL BE LOOSE

Calibration of the complete system uses a second-order curve of the form

$$T = a_o + a_1 V_{out} + a_2 V^2_{out}$$

where

T = temperature at °C

a_o, a_1, and a_2 = voltage coefficients

V_{out} = amplifier output (volts dc)

The curve form of calibration is necessary because of the nonlinearity of the temperature sensor material over the temperature range of interest and the necessity of supplying the required accuracy. This material varies in resistance according to the Callendar - Van Dusen equation which gives the second-order calibration curve above. The required accuracy in this equation is obtained by using the appropriate constants from Table 4.

Table 4

TEMPERATURE SENSOR - AMPLIFIER CALIBRATION

NOTE: (All amplifiers interchangeable with any temperature sensor system)

(Amplifier Scale Factor = 366.41)

Temperature Sensor S/N	Amplifier Output at -55°C (volts dc)	Amplifier Output at 0°C (volts dc)	Amplifier Output at +45°C (volts dc)	Voltage Coefficients		
				a_o	a_1	a_2
001	-0.003	2.924	5.002	-54.949	17.119	0.5724
002	0.005	2.926	5.000	-55.086	17.146	0.5742
003	0.001	2.929	5.004	-55.017	17.084	0.5802
004	0.001	2.926	4.999	-55.017	17.103	0.5811
005	0.002	2.924	4.998	-55.034	17.139	0.5754
006	0.000	2.924	5.000	-55.000	17.134	0.5733
008	-0.001	2.927	5.005	-54.983	17.106	0.5736
009	0.004	2.927	5.002	-55.069	17.133	0.5743
010	0.003	2.925	5.001	-55.051	17.151	0.5709
011	0.001	2.926	5.003	-55.017	17.128	0.5723
012	0.001	2.924	4.998	-55.017	17.130	0.5765
014	0.002	2.925	5.001	-55.034	17.142	0.5721
015	0.000	2.924	4.997	-55.000	17.114	0.5799
016	0.003	2.925	4.999	-55.051	17.138	0.5754

NOTE: To obtain a temperature at a voltage, substitute given values of coefficients into formula:

$$T = a_o + a_1 V_{out} + a_2 V^2_{out}$$

where T = Temperature (°C); a_o, a_1, a_2, = voltage coefficient; V_{out} = Amplifier output (volts dc).

Section 5
FABRICATION OF FINAL RADOME

The radome was layed up in the mold shown in Figure 16 using Fibco Plastics First Article Inspection sheets shown as Figure 17.

To ensure fit of the final radome to the particular P3A aircraft, Fibco Plastics was directed to make a layup of the nose section of the aircraft. This resulted in a jig (Figure 18) from which the male mold was made. The final radome was cut and trimmed in this jig.

At time of inspection, probe holes were cut along the lines shown in Figure 19. There is a 40-in.-wide window area in which the thickness was carefully controlled. The holes matched the lines on which the lightning arresters were later placed. Inspection was both by MDAC inspection personnel and government personnel represented by Defense Contract Administration Services. Fibco Plastic Part Inspection Report (Figure 20) shows the final dimensions attained.

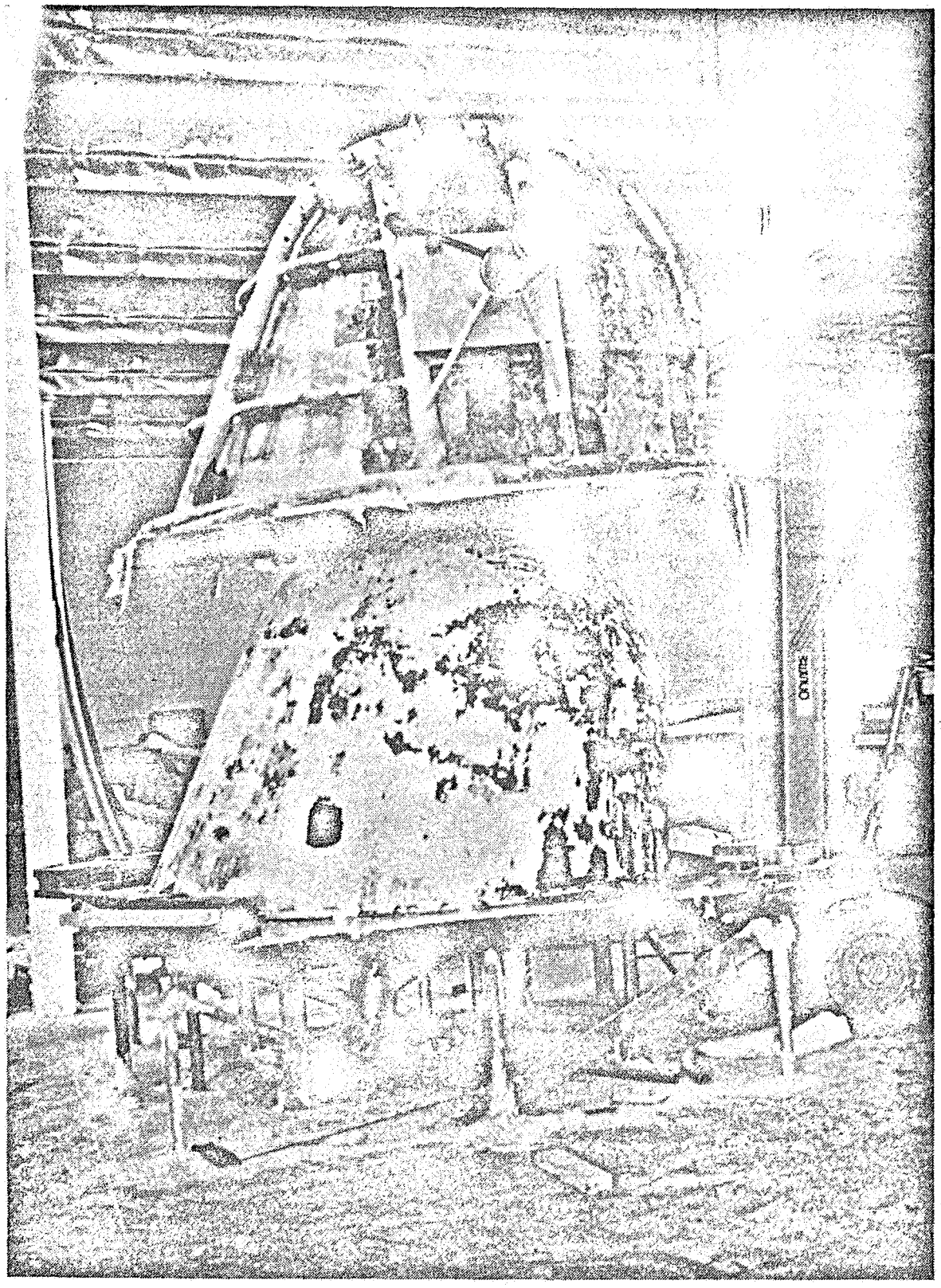

Figure 16. Radome Mold

Sheet 1 of 4

FIBCO PLASTICS, INC.
FIRST ARTICLE INSPECTION
AND/OR
PART INSPECTION REPORT

CUSTOMER McDonnell Douglas DATE 4-4-69
CUSTOMER'S PART NO. S/O 175098-10 L.S.-2099-A REVISION
PART NAME Radome P.O. NO. S/O 175098-10 L.S.-2099-A
FPI W.O. NO. INSPECTOR PART SERIAL # 1

BLUEPRINT CALLOUT AND TOLERANCE	ACTUAL DIMENSIONS	IN TOL.	OUT TOL.	REMARKS
Resin 828 Shell Chemicals Batch 1RLHJ10				
Catalyst Curing Agent "A" Ram Chemical Batch 8F192				
1st Stage				
Window Area				
1 Layer 1581 X 60	Lot #739900			
1 Layer 1581 X 50	Lot #515043			
1 Layer 1584 X 60	Lot #549841			
Total weight of cloth	34.00 lbs.			
resin	13.222 lbs.			
catalyst	1.0577 lbs.			
Cure for 2 hrs. at	200°F.			

APPROVED BY

NOTICE TO OFFICE:
[illegible] receipt of this APPROVED form you are authorized to invoice

Figure 17. Subcontractor First Article Inspection

Sheet 2 of 4

FIBCO PLASTICS, INC.
FIRST ARTICLE INSPECTION
AND/OR
PART INSPECTION REPORT

CUSTOMER McDonnell Douglas DATE 4/5/89

CUSTOMER'S PART NO. S/O 175098-10 L.S.-2099-A REVISION

PART NAME Radome P.O. NO. S/O 175098-10 L.S.-2099-A

FPI W.O. NO. _____ INSPECTOR _____ PART SERIAL # 1

BLUEPRINT CALLOUT AND TOLERANCE	ACTUAL DIMENSIONS	IN TOL.	OUT TOL.	REMARKS
Resin 828 Shell Chemicals Batch 12LKJ10				
Catalish Curing Agent "A" Ems Chemical Batch BF198				
2nd Stage				
1 Layer 1584 X 50	Lot #529812			
1 Layer 1584 X 60	Lot #548041			
1 Layer 1584 X 50	Lot #529812			
Total weight of cloth	57.00 lbs.			
resin	22.1666 lbs.			
catalist	1.773 lbs.			
Cure for 2 hrs. at	200°F.			

APPROVED BY [signature]

NOTICE TO OFFICE:
Upon receipt of this APPROVED form you are authorized to invoice.

Figure 17. Subcontractor First Article Inspection (Cont.)

Sheet 3 of 4

FIBCO PLASTICS, INC.
FIRST ARTICLE INSPECTION
AND/OR
PART INSPECTION REPORT

CUSTOMER McDonnell Douglas DATE 4-7-69
CUSTOMER'S PART NO. S/O 175033-10 L.S.-2099-A REVISION
PART NAME Radome P.O. NO. S/O 175033-10 L.S.-2099-A
FPI W.O. NO. INSPECTOR PART SERIAL # 1

BLUEPRINT CALLOUT AND TOLERANCE	ACTUAL DIMENSIONS	IN TOL.	OUT TOL.	REMARKS
Resin 828 Shell Chemicals Batch 12LEV10				
Catalist Curing Agent "A" Ram Chemical Batch 87192				
3rd Stage				
Window Area				
1 Layer 1534 X 60	Lot 6549841			
1 Layer 1534 X 90	Lot 6529812			
1 Layer 1534 X 60	Lot 6549841			
Total weight of cloth	62.00 lbs.			
resin	24.111 lbs.			
catalist	1.6286 lbs.			
Cure for 2 hrs. at	200°F.			

APPROVED BY

NOTICE TO OFFICE:
Upon receipt of this APPROVED form you are authorized to invoice.

Figure 17. Subcontractor First Article Inspection (Cont.)

Sheet 4 of 6

FIBCO PLASTICS, INC.
FIRST ARTICLE INSPECTION
AND/OR
PART INSPECTION REPORT

CUSTOMER McDonnell Douglas DATE 4-8-68
CUSTOMER'S PART NO. S/O 175098-10 L.S.-2099-A REVISION
PART NAME Radome P.O. NO. S/O 175098-10 L.S.-2099-A
FPI W.O. NO. INSPECTOR PART SERIAL # 1

BLUEPRINT CALLOUT AND TOLERANCE	ACTUAL DIMENSIONS	IN TOL.	OUT TOL.	REMARKS
1 [illegible] Chemicals Batch 121-EJ10				
[illegible] Agent "A" Ram Chemical Batch 8F192				
4th STAGE				
Window Area				
1 Layer 1584 X 50"	Lot [illegible]			
1 Layer 1581 X 60"	Lot [illegible]			
1 Layer 1581 X 50"	Lot [illegible]			
Total weight of cloth	56.00 lbs.			
Resin	21.777 lbs.			
Catalyst	1.7421 lbs.			
Cure for 2 hrs. at	200°F.			

APPROVED BY

NOTICE TO OFFICE: [illegible] are authorized to invoice

Figure 17. Subcontractor First Article Inspection (Cont.)

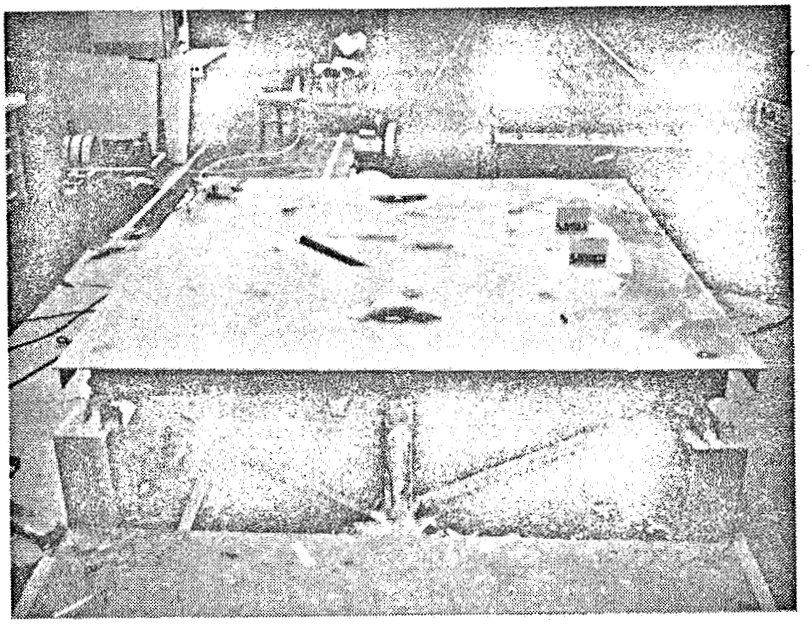

Figure 18. Radome Interface Jig

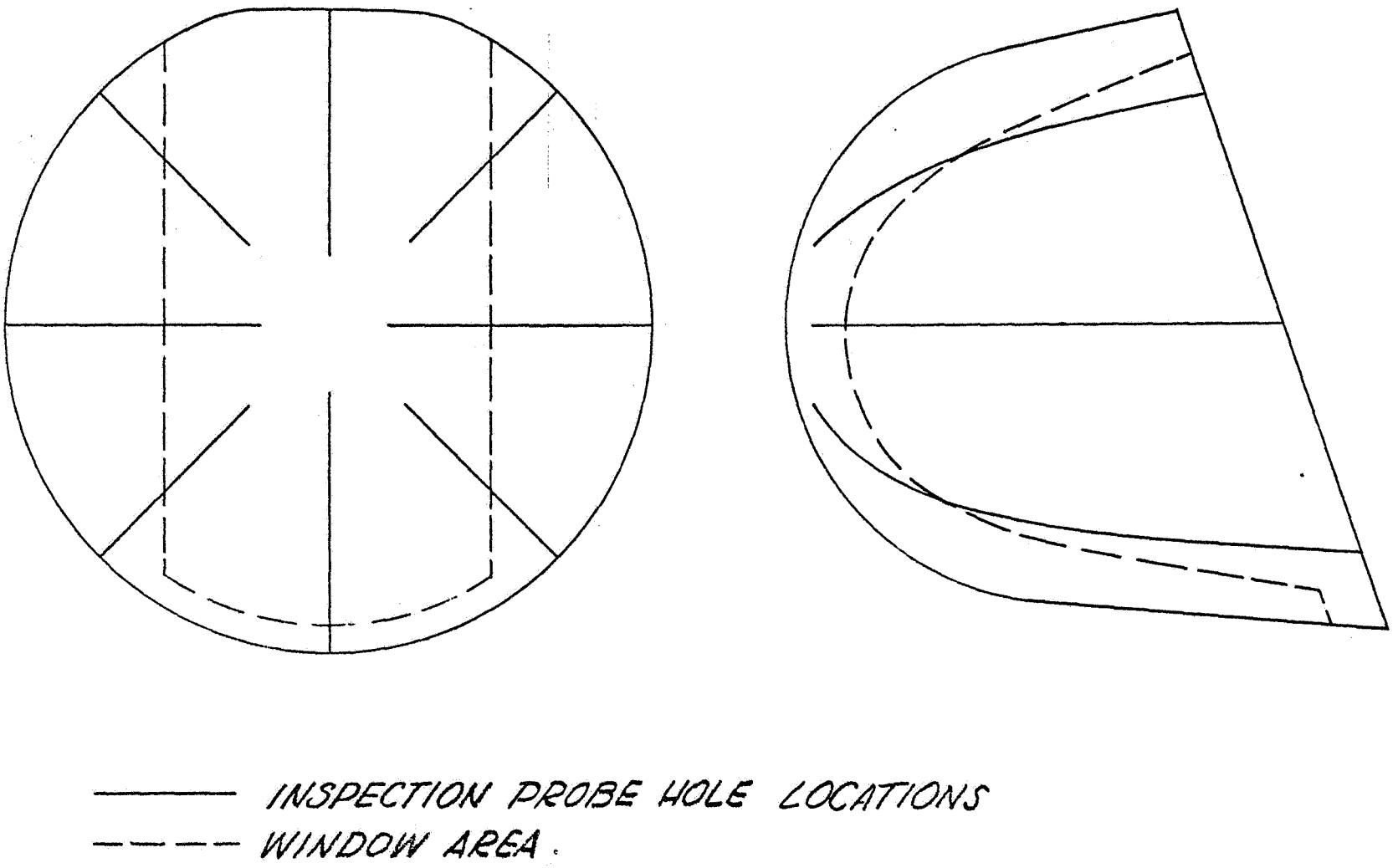

Figure 19. Thickness Measurement Points

Sheet 1 of 2

FIBCO PLASTICS, INC.
FIRST ARTICLE INSPECTION
AND/OR
PART INSPECTION REPORT

CUSTOMER McDonnell Douglas DATE 4-16-69
CUSTOMER'S PART NO. S/O 175098-10 L. S.-2099-A REVISION
PART NAME Radome P.O. NO. S/O 175098-10 L.S.-2099-A
FPI W.O. NO. INSPECTOR PART SERIAL # 1
9D17

BLUEPRINT CALLOUT AND TOLERANCE		ACTUAL DIMENSIONS	IN TOL.	OUT TOL.	REMARKS
Location A	1	.270	OK		.258 - .272 Allowable
	2	.269	OK		
	3	.265	OK		
	4	.261	OK		
	5	.260	OK		
	6	.264	OK		
	7	.265	OK		
	8	.270	OK		
	9	.267	OK		
	10	.260	OK		
	11	.268	OK		
	12	.270	OK		
	13	.272	OK		
Location B	1	.265	OK		
	2	.270	OK		
	3	.272	OK		
Location C	1	.265	OK		
Location D	1	.268	OK		
	2	.266	OK		
	3	.266	OK		
Location E	1				
	2	.264	OK		
	3	.271	OK		
	4	.270	OK		
	5	.267	OK		
	6	.263	OK		
	7	.272	OK		
	8	.260	OK		
	9	.269	OK		
	10	.272	OK		
	11	.265	OK		

APPROVED BY

NOTICE TO OFFICE:
... this APPROVED form you are authorized to invoice.

Figure 20. Subcontractor Part Inspection Report

Sheet 2 of 2

FIBCO PLASTICS, INC.
FIRST ARTICLE INSPECTION
AND/OR
PART INSPECTION REPORT

CUSTOMER McDonnell Douglas DATE 4-16-69
CUSTOMER'S PART NO. S/O 175088-10 L.S.-2099-A REVISION
PART NAME Endcone P.O. NO. S/O 175088-10 L.S.-2099-A
FPI W.O. NO. INSPECTOR DAC 9D17 PART SERIAL # 1

BLUEPRINT CALLOUT AND TOLERANCE		ACTUAL DIMENSIONS	IN TOL.	OUT TOL.	REMARKS
Location F	1	.277			.258 - .272 allowable
	2	.265	OK		
	3	.269	OK		
Location G	1	.270	OK		
Location H	1	.263	OK		
	2	.260	OK		
	3	.259	OK		

APPROVED BY

NOTICE TO OFFICE: ... approval form you are authorized to invoice.

Figure 20. Subcontractor Part Inspection Report (Cont.)

Section 6
MEASUREMENTS

Two categories of tests were made on the radiometer system which included both radomes: (1) pattern tests at the MDAC Microwave Test Site, and (2) transmission tests at both MDAC and Table Mountain (JPL). A complete set of patterns was obtained. Radome 1 was measured for both horizontal and vertical polarization transmission loss. Radome 2 was measured for only horizontal polarization losses due to lack of time.

6.1 PATTERN TESTS

Side-lobe levels, beamwidth change, and beam deflection were measured from the recorded patterns and are presented in Tables 5 through 21. These tables summarize the significant information taken from the patterns and put in a form from which comparisons can be made. The raw data representing 226 pattern recordings were taken at a sufficient scale on the recorder to give the necessary angular accuracy required by the specification. Approximately 1,000 feet of Scientific Atlanta Recording Paper 121 were used and because of this bulk, patterns have not been included in this report. The original patterns are being forwarded to MSC at no additional cost to the government.

These tables and the following comments on patterns use Figure 21. The four antennas are oriented so that the electric vector for each antenna is in the same plane. This is called the E-plane in the text and is shown in Figure 21. The plane at right angles is called the H-plane. Since the complete antenna package can rotate, it follows that the E-plane can be oriented at any angle with respect to the earth. However, system operation has the antenna package in one of two positions represented by Figure 21a (1) or (2) and called accordingly horizontal or vertical polarization.

Table 5

SUMMARY FOR ELEVATION PATTERNS, HORIZONTAL POLARIZATION AT 1.42 GHz

Radome	Angle (deg)	Beam Width (deg)	Bottom Side Lobes (dB/angle in deg)	Top Side Lobes (dB/angle in deg)		Pattern No.
1	0	17.2	15/24	17/24	15/34	27
	30	15.5	14/26	13/30		29
	70	14.8	13/26	Not available		31
	160	14.0	13/26	12/34		33
Free Space	0	14.6	14/24	20/28	19/36	59
	30	14.6	14/24	22/24	21/34	61
	70	14.2	13/24	Not available		63
	160	14.6	12/22	20/30		65
2	0	17.5	18/24	19/26	20/36	195
	30	15.4	15/24		14/36	197
	70	14.5	14/24	Not available		199
	160	13.2	15/22	16/36		201

Table 6

SUMMARY FOR AZIMUTH PATTERNS, HORIZONTAL POLARIZATION AT 1.42 GHz

Radome	Angle (deg)	Beam Width (deg)	Beam Center (deg)	90° Side Lobes (dB/angle in deg)		270° Side Lobes (dB/angle in deg)			Pattern No.
1	0	16.6	-0.3	19/32	-*	25/34	23/60		28
	30	14.8	-0.1	21/34	26/60	23/22	24/36	24/60	30
	70	14.3	-0.05	18/34	26/58	22/22	22/34	22/54	32
	160	15.3	-1.65	21/36		28/22	25/34	25/54	34
Free Space	0	15.9	-0.25	19/34	-	22/34	27/60		60
	30	16.1	-0.05	20/36		22/34	28/60		62
	70	15.8	-0.3	20/34		22/32	29/60		64
	160	15.9	-1.35	19/36		22/32	28/60		66
2	0	16.2	-0.3	19/34	25/60	26/34	23/60		196
	30	15.1	+0.05	18/34	27/60	22/34	23/60		198
	70	15.0	-0.1	19/34		23/34	23/60		200
	160	15.5	-1.25	23/36	-	25/34	24/60		202

*- means more than 30 dB

Table 7

SUMMARY FOR ELEVATION PATTERNS, VERTICAL POLARIZATION AT 1.42 GHz

Radome	Angle (deg)	Beam Width (deg)	Bottom Side Lobes (dB/angle in deg)		Top Side Lobes (dB/angle in deg)		Pattern No.
1	0	15.8		22/36	20/34		131
	30	15.0	24/24	24/34	22/34		133
	70	14.8	23/34		Not available		135
	160	15.1	22/34		23/34		137
Free Space	0	16	22/32		19/34		107
	30	16.1	22/34		20/36		109
	70	15.7	22/34		Not available		111
	160	16.0	22/30		21/36		113
2	0	14.4	21/34		18/26	20/36	171
	30	14.8	22/36		19/32		173
	70	14.6	24/36		Not available		175
	160	15.1	23/32		23/34		177

Table 8

SUMMARY FOR AZIMUTH PATTERNS, VERTICAL POLARIZATION AT 1.42 GHz

Radome	Angle (deg)	Beam Width (deg)	Beam Center (deg)	90° Side Lobes (dB/angle in deg)			270° Side Lobes (dB/angle in deg)			Pattern No.
1	0	14.2	-0.4	13/22	20/42	23/60	18/26	20/48		132
	30	14.3	-0.35	14/22	23/42	—*		15/34		134
	70	14.8	-0.1	13/22	22/42	23/52		14/32		136
	160	14.9	-1.05	14/24	23/44	23/60		14/30		138
Free Space	0	14.9	+0.25	13/24	20/42	25/60	20/24	21/36	20/54	108
	30	14.6	+0.3	14/24	20/42	25/60	20/24	21/36	21/54	110
	70	14.2	+0.25	14/24	21/38	26/60	21/24	21/36	22/54	112
	160	14.6	-0.05	14/24	21/42	25/60	21/24	21/36	22/54	114
2	0	14.1	-0.15	14/24	20/30	23/60	15/28	-		172
	30	14.6	-0.35	14/24	22/30	-	14/34	21/60		174
	70	14.7	-0.15	13/22	23/30	-	15/32	24/60		176
	160	14.5	-1.25	14/24	20/34	24/60	14/28	-		178

*- means more than 30 dB

Table 9

SUMMARY FOR ELEVATION PATTERNS, HORIZONTAL POLARIZATION AT 10.6 GHz

Radome	Angle (deg)	Beam Width (deg)	Bottom Side Lobes (dB/angle in deg)	Top Side Lobes (dB/angle in deg)	Pattern No.
1	0	4.9	27/14 -* 30/24 - 30/42	29/10 28/20	51
	30	4.8	26/14 29/20 - - 28/42	28/10 25/18	53
	70	4.7	25/14 30/20 - - 29/36 -	Not available	55
	160	4.8	25/12 21/20 26/24 23/30 23/36 23/40	22/8 S** 23/20 20/24 24/36	57
Free Space	0	5.2	31/8 28/14	28/10 26/20	83
	30	5.2	32/12 27/14	28/10 26/18	85
	70	4.9	31/10 27/14	Not available	87
	160	5.1	31/8 27/12 30/18 29/20 29/36	28/12 27/22	89
2	0	4.9	27/14	28/10 25/20	187
	30	4.9	27/14 - -	30/10 26/20	189
	70	4.9	27/14 - -	Not available	191
	160	4.7	22/10 27/14 25/18 22/24 21/32	S 20/14 21/18 26/22 22/28	193

*- means more than 30 dB

**S = Shoulder

Table 10

SUMMARY FOR AZIMUTH PATTERNS, HORIZONTAL POLARIZATION AT 10.6 GHz

Radome	Angle (deg)	Beam Width (deg)	Beam Center (deg)	90° Side Lobes (dB/angle in deg)	270° Side Lobes (dB/angle in deg)	Pattern No.
1	0	4.8*	+0.2	21/8^{S} 27/18 29/36 -**	20/8^{S}*** 29/12 26/18	52
	30	4.8	+0.35	19/8^{S} 28/18 30/28 30/36	19/8^{S} 28/12 26/18	54
	70	4.8	+0.35	21/8^{S} 30/18 - 29/36	21/8^{S} 29/18	56
	160	4.8	+0.6	22/8 28/20 27/24 27/28 27/34	18/8^{S} 27/14 23/18 27/40	58
Free Space	0	5.0*	+0.2	21/8^{S} 29/16 29/38	21/8^{S} 28/16	84
	30	4.9	+0.25	21/8^{S} 29/14 29/36	21/8^{S} 28/16	86
	70	4.9	+0.25	21/8^{S} 29/14 29/36	21/8^{S} 27/18	88
	160	4.9	+0.45	21/7^{S} 28/16	21/8^{S} 29/16	90
2	0	4.8	+0.4	20/8^{S} 28/18	20/8^{S} 27/18	188
	30	4.7	+0.41	20/8^{S} 28/18	21/8^{S} 28/18	190
	70	4.8	+0.4	20/6^{S} 29/12 27/18	20/8^{S} 26/18	192
	160	4.6*	-0.7	19/8 20/14 25/40	19/6 22/12 25/18 23/26 26/32	194

*Notch

**- means more than 30 dB

***S = Shoulder

Table 11

SUMMARY FOR ELEVATION PATTERNS, VERTICAL POLARIZATION AT 10.6 GHz

Radome	Angle (deg)	Beam Width (deg)	Bottom Side Lobes (dB/angle in deg)				Top Side Lobes (dB/angle in deg)				Pattern No.
1	0	4.8	19/7^{S**}	-*	-		22/7^{S}	-	-		123
	30	4.8	20/8^{S}	25/18			22/6^{S}	26/16			125
	70	4.8	21/8^{S}	30/18			21/6^{S}				127
	160	4.9	23/6^{S}	25/16			20/8^{S}	26/16			129
Free Space	0	4.8	21/8^{S}	29/16			21/8^{S}				91
	30	4.8	21/8^{S}	29/18			21/6^{S}				93
	70	4.8	21/8^{S}	29/18			21/6^{S}				95
	160	4.7	21/6^{S}	27/14			21/8^{S}				97
2	0	4.9	20/8^{S}	28/18	-		22/8^{S}	28/12	29/18	27/28	179
	30	4.8	21/8^{S}	31/18	-	-	21/6^{S}	29/14	-		181
	70	4.7	20/8^{S}	27/18			21/6^{S}	Not available			183
	160	4.9	S	30/10	27/14	28/36	23/8^{S}	31/16	-	-	185

*- means more than 30 dB

**S = Shoulder

Table 12

SUMMARY FOR AZIMUTH PATTERNS, VERTICAL POLARIZATION AT 10.6 GHz

Radome	Angle (deg)	Beam Width (deg)	Beam Center (deg)	90° Side Lobes (dB/angle in deg)	270° Side Lobes (dB/angle in deg)	Pattern No.
1	0	4.9	+0.35	25/10 26/12 28/20 26/54	25/10 24/20 28/54	124
	30	4.8*	+0.35	26/12 27/14 24/54	26/10 26/20	126
	70	5.2**	-0.5	26/14 28/22	26/10 26/20	128
	160	4.8**	-0.7	20/14 23/26 15/60	22/6 21/18 25/54 27/78	130
Free Space	0	4.9*	-0.15	28/14	28/12 26/20	92
	30	4.9*	-0.15	28/14	28/12 26/20	94
	70	5.0**	-0.1	28/12	28/12 26/20	96
	160	5.0*	+0.9	28/10 26/20	28/14	98
2	0	4.9	+0.95	S*** 29/14 25/60	S 23/20 - -	180
	30	4.9**	+0.65	31/8 26/12 24/14 23/54	27/10 25/12 24/22	182
	70	4.9	+0.15	31/8 26/14 - - -	27/14 25/20 - -	184
	160	4.9*	-0.75	25/8S 25/14 27/16 25/24 22/28 20/60 21/62	24/8 24/10 22/20 27/24 26/32 25/52	186

*Notch

**Flat top

***S = Shoulder

Table 13

SUMMARY FOR ELEVATION PATTERNS, HORIZONTAL POLARIZATION AT 22.3 GHz

Radome	Angle (deg)	Beam Width (deg)	Bottom Side Lobes (dB/angle in deg)			Top Side Lobes (dB/angle in deg)				Pattern No.
1	0	5.3	22/10	23/16	26/20	22/10	22/16			35
	30	4.9	22/10	22/16	23/20	22/10	25/14	26/30		37
	70	4.9	20/12	22/16	26/22	Not available				39
	160	5.1	22/10	23/14	22/16	22/10	26/16			41
Free Space	0	5.3	22/10	24/16	27/20	23/10	26/16	27/20	26/30	67
	30	5.1	23/10	24/16	28/20	24/10	27/14	28/20	28/30	69
	70	5.3	23/9	25/16	28/22	Not available				71
	160	5.1	23/9	25/14	29/19	25/12	28/16	28/22	28/32	73
2	0	5.2	21/10	24/16	26/20	22/10	24/16	24/20	25/30	203
	30	5.6	22/10	23/16	26/22	22/10	24/14	25/20	24/28	205
	70	5.5	18/10	21/16	26/22	Not available				207
	160	5.6	20/14	24/18	25/24	24/12	24/18	26/22		209

Table 14

SUMMARY FOR AZIMUTH PATTERNS, HORIZONTAL POLARIZATION AT 22.3 GHz

Radome	Angle (deg)	Beam Width (deg)	Beam Center (deg)	90° Side Lobes (dB/angle in deg)	270° Side Lobes (dB/angle in deg)	Pattern No.
1	0	4.9*	+0.65	18/8S*** 24/16 26/22	21/9S 26/18 27/22	36
	30	4.8	+0.7	19/7S 25/16 26/22	21/9S 25/18 26/22	38
	70	4.7*	+0.45	18/7S 24/16 28/22	19/8S 26/14 25/18 26/22	40
	160	4.8*	+0.1	17/7S 24/13 24/16	18/8S 21/16	42
Free Space	0	4.8	+0.3	20/8S 30/13 26/17 28/22	21/8S 27/14 26/18 27/22	68
	30	4.9**	+0.45	19/8S 28/13 26/16 28/22	20/8S 27/14 26/18 26/22	70
	70	5.0	+0.5	19/8S 29/13 26/16 28/22	20/8S 27/14 26/18 27/22	72
	160	4.9*	-0.55	20.9S 29/14 26/18 28/23	21/8S 28/14 26/16 27/22	74
2	0	5.4*	+1.1	18/8S 25/12 22/18 24/22	20/8S 24/18 23/22	204
	30	5.4**	+0.85	17/8S 23/16 26/22	19/8S 26/14 24/18 24/22	206
	70	5.3	+0.75	18/8S 28/12 22/16 27/22	20/8S 25/14 25/18 24/22	208
	160	5.7**	-0.35	15/8S 27/12 21/18 23/22	19/8S 22/14 20/16	210

*Notch

**Flat top

***S = Shoulder

Table 15

SUMMARY FOR ELEVATION PATTERNS, VERTICAL POLARIZATION AT 22.3 GHz

Radome	Angle (deg)	Beam Width (deg)	Bottom Side Lobes (dB/angle in deg)				Top Side Lobes (dB/angle in deg)			Pattern No.
1	0	4.8	$18/10^{S*}$	24/14	23/27		$17/8^{S}$	23/16	25/22	139
	30	4.9	$19/10^{S}$	26/14	25/18	25/23	$18/6^{S}$	23/16	23/20	141
	70	4.9	$19/10^{S}$	26/14	26/18	26/24	$21/8^{S}$	Not available		143
	160	4.9	$20/8^{S}$	25/12	25/16	24/20	$20/9^{S}$	27/18	27/22	145
Free Space	0	4.8	$20/9^{S}$	27/14	26/18	26/22	$19/8^{S}$	26/16	28/22	115
	30	4.9	$20/9^{S}$	27/14	26/18	26/22	$19/7^{S}$	26/16	28/22	117
	70	5.0	$20/9^{S}$	27/14	26/18	26/22	$20/7^{S}$	Not available		119
	160	5.2	$20/9^{S}$	27/14	26/18	26/22	$19/7^{S}$	25/18	27/23	121
2	0	4.7	$17/8^{S}$	25/14	24/18	27/22	$18/8^{S}$	25/16	25/22	163
	30	4.7	$18/10^{S}$	25/14	26/18	26/24	$19/8^{S}$	24/16	26/22	165
	70	4.7	$20/8^{S}$	26/14	26/18	25/24	$19/7^{S}$	Not available		167
	160	4.8	$20/7^{S}$	27/12	26/16	26/22	$20/9^{S}$	25/18	27/22	169

*S = Shoulder

Table 16

SUMMARY FOR AZIMUTH PATTERNS, VERTICAL POLARIZATION AT 22.3 GHz

Radome	Angle (deg)	Beam Width (deg)	Beam Center (deg)	90° Side Lobes (dB/angle in deg)	270° Side Lobes (dB/angle in deg)	Pattern No.
1	0	5.4*	+0.8	21/10 22/14 18/36	24/14 21/20	140
	30	5.2**	+0.8	24/8 23/14 26/18	26/10 29/16 25/20	142
	70	5.1	+0.55	21/10 28/20	29/12 29/16 26/20	144
	160	5.1	-0.35	23/10 24/14	27/10 24/20	146
Free Space	0	5.1	+0.05	23/10 25/14 28/20	24/10 27/16 28/30	116
	30	5.1**	+0.05	23/10 24/14 -	24/10 27/16 28/30	118
	70	5.0**	+0.2	22/10 24/14 -	23/10 27/16 27/30	120
	160	5.1	-0.05	23/10 27/16 28/20 27/30	22/10 23/16 27/20	122
2	0	5.1**	+0.55	22/10 23/14 26/20	22/12 26/16 25/20	164
	30	5.3	+1.25	19/8S*** 23/16 22/20	22/12 25/16 26/20 27/30	166
	70	4.9*	+0.65	23/10 24/14 28/20	24/14 27/16 28/20 28/30	168
	160	5.1*	-0.25	21/10 25/16 26/20	21/10 25/14 26/18 26/26 26/30	170

*Flat top

**Notch

***S = Shoulder

Table 17

SUMMARY FOR ELEVATION PATTERNS, HORIZONTAL POLARIZATION AT 31.4 GHz

Radome	Angle (deg)	Beam Width (deg)	Bottom Side Lobes (dB/angle in deg)	Top Side Lobes (dB/angle in deg)	Pattern No.
1	0	5.1	22/10 27/20	22/12 25/36	43
	30	5.0	23/10$^{\Delta}$ 25/20	21/10 26/36	45
	70	5.3	23/12$^{\Delta}$ 25/20	Not available	47
	160	6.4	22/12 25/18	24/8$^{\Delta}$ 25/16 24/36	49
Free Space	0	5.9	26/14 28/24	26/14 28/18 26/22	75
	30	5.9	26/14 28/24	25/12 28/18 26/22	77
	70	5.9	25/14 27/24	Not available	79
	160	6.1	25/12 26/20	24/14 28/20 25/24	81
2	0	5.7	19/8$^{\Delta}$ 23/14 23/22	24/12$^{\Delta}$ 24/14$^{\Delta}$	211
	30	5.9	27/14$^{\Delta}$ 28/24$^{\Delta}$	26/14$^{\Delta}$ 28/24	213
	70	5.7	24/14 27/24	Not available	215
	160	6.3	26/12 27/22	23/14 28/26	217

$^{\Delta}$has a 2 to 3 dB ripple on it

Table 18

SUMMARY FOR AZIMUTH PATTERNS, HORIZONTAL POLARIZATION AT 31.4 GHz

Radome	Angle (deg)	Beam Width (deg)	Beam Center (deg)	90° Side Lobes (dB/angle in deg)	270° Side Lobes (dB/angle in deg)	Pattern No.
1	0	5.3	+0.05	27/8^{S}	27/18	44
	30	5.1	+0.15	24/8^{S} -	26/18	46
	70	5.1	+0.15	23/8^{S} -	28/16 -	48
	160	5.3*	-1.35	21/8^{S} 24/36	19/6^{S} 25/16 19/34	50
Free Space	0	5.3**	+0.15	20/8^{S}	29/18	76
	30	5.7*	+0.35	20/8^{S}	28/18	78
	70	5.4**	+0.3	19/8^{S} 29/16	28/18	80
	160	5.2**	+0.4	28/16 - -	20/8 - -	82
2	0	5.4	+0.3	20/8^{S} 29/20$^{\Delta}$	S$^{\Delta}$ 26/18$^{\Delta}$ 26/36$^{\Delta}$	212
	30	5.5	+0.45	19/8^{S} - -	- 28/18	214
	70	5.4	+0.1	18/6^{S} 29/18$^{\Delta}$	27/18$^{\Delta}$	216
	160	6.1**	-0.65	18/10^{S} 25/18 25/22	17/8 23/14 23/18	218

*Flat top

**Notch

$^{\Delta}$2 dB ripple

Table 19

SUMMARY FOR ELEVATION PATTERNS, VERTICAL POLARIZATION AT 31.4 GHz

Radome	Angle (deg)	Beam Width (deg)	Bottom Side Lobes (dB/angle in deg)				Top Side Lobes (dB/angle in deg)			Pattern No.
1	0	5.2	-	-	22/36		$18/8^S$	-		147
	30	4.8	$19/8^S$		27/18		$17/8^S$	-		149
	70	5.1			26/18		$19/8^S$	Not available		151
	160	5.1	19/8	23/12	25/14		$19/8^S$	25/20		153
Free space	0	5.1	27/18	29/28			$20/8^S$	-	-	99
	30	5.1	27/18	29/28			$20/8^S$	-	-	101
	70	5.2	28/18	30/28			$21/8^S$	Not available		103
	160	5.1	28/18	30/26			$21/8^S$	-	-	105
2	0	5.2	24/10	28/16	25/36		$20/8^S$	-		155
	30	5.0	-	27/18	28/28	27/34	$20/8^S$	28/14	-	157
	70	5.1	28/12	26/18			$18/8^S$	Not available		159
	160	5.9	26/10	25/12	23/14		$18/10^S$	-	-	161

Table 20

SUMMARY FOR AZIMUTH PATTERNS, VERTICAL POLARIZATION AT 31.4 GHz

Radome	Angle (deg)	Beam Width (deg)	Beam Center (deg)	90° Side Lobes (dB/angle in deg)				270° Side Lobes (dB/angle in deg)			Pattern No.
1	0	5.7*	+1.25	24/12	27/22			26/14	-		148
	30	5.5**	+1.75	25/12	28/22			24/14	25/26		150
	70	5.6*	+1.2	25/12	28/22			24/14	25/24		152
	160	5.9**	+0.65	19/14	23/18	23/22	20/36	21/12	21/22		154
Free Space	0	5.6**	+0.8	27/12	29/24			26/14S	29/20	28/24	100
	30	5.6**	+0.7	27/14	29/24			26/14S	29/20	28/24	102
	70	5.5**	+0.75	27/14	29/24			25/14S	29/20	28/24	104
	160	5.5*	-0.15	26/14	28/24			27/14	29/24		106
2	0	5.5*	+1.65	25/12	26/22			26/14	28/20		156
	30	5.6*	+1.2	26/12	28/22	-		25/12	26/24	-	158
	70	5.6	+1.05	26/12	28/18	27/22	-	24/14	25/24	-	160
	160	6.3*	-0.45	24/10	19/14	21/16		19/12	22/16	21/18	162

*Flat top

**Notch

Table 21

SUMMARY FOR PATTERNS TAKEN WITHOUT LIGHTNING ARRESTERS, RADOME 2
HORIZONTAL POLARIZATION AT 22.3 GHz

Pattern	Angle (deg)	Beam Width (deg)	Bottom Side Lobes (dB/angle in deg)				Top Side Lobes (dB/angle in deg)				Pattern No.
Elevation	0	4.9*	23/10$^{\Delta}$	25/14$^{\Delta}$	27/20$^{\Delta}$		23/10$^{\Delta}$	27/16$^{\Delta}$	26/20$^{\Delta}$		219
	30	5.2	23/10$^{\Delta}$	23/16$^{\Delta}$			23/10$^{\Delta}$	26/16$^{\Delta}$	26/20$^{\Delta}$		221
	70	5.2	20/10	24/16	25/20		Not available				223
	160	5.0**	21/6$^{\Delta}$	23/14$^{\Delta}$	26/18$^{\Delta}$		25/12	25/18	27/70		225
			90° Side Lobes				270° Side Lobes				
Azimuth	0	5.1	18/8^{S}	22/16	25/22		20/8^{S}	25/18	23/22		220
	30	4.9	18/8^{S}	25/10	-		20/8^{S}	27/14	25/18	25/24	222
	70	4.9	18/8^{S}	23/16	-		19/8^{S}	26/14	26/18	24/22	224
	160	5.3**	17/8^{S}	24/14	24/22	24/42	21/8^{S}	25/14	25/16		226

*Notch

**Flat Top

2-3 dB ripple = Δ

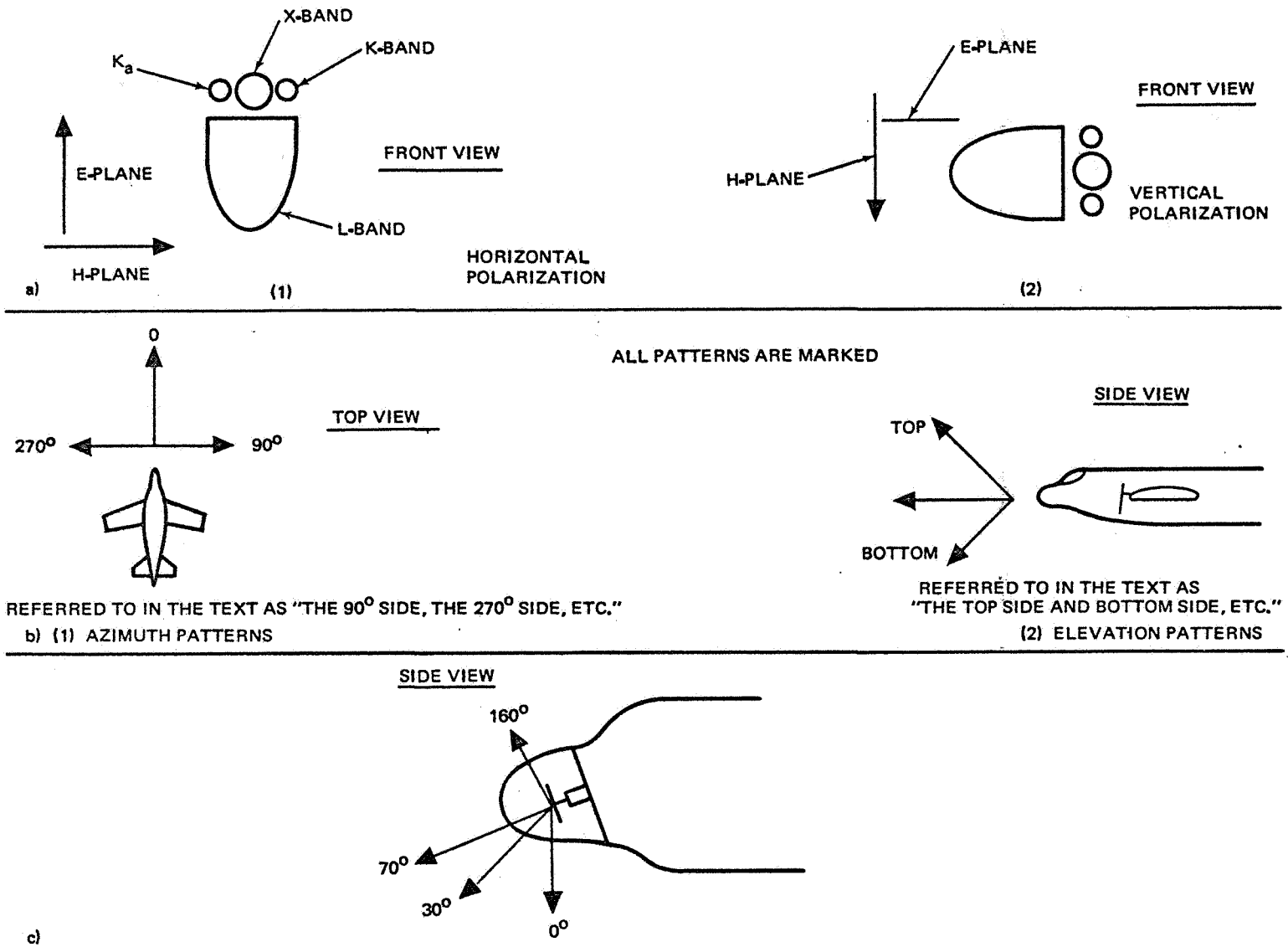

Figure 21. Geometry of System

Each pattern as recorded uses the nomenclature of Figure 21 and is so marked. Figure 21 shows the four discrete angles for which the azimuth and elevation patterns were taken. Figure 22 shows the antenna package on the test pedestal and corresponds in oriental to Figure 21a (1).

The elevation plane of the antenna package is skewed with respect to the plane of the mount elevation table. Therefore, patterns taken in the azimuth plane should be given more weight than those taken in the elevation plane. Variations in the symmetry of the main beam are considered from the azimuth plane patterns only. Notches and flat tops occurred on the main beam for innumerable patterns at X-, K-, and K_a-bands. Some examples of these variations are shown in Figure 23.

Comparisons from the patterns are made for the following cases: (1) with and without lightning arresters, (2) variation in side-lobe levels, (3) variation in beam shift, and (4) variation in beam-width.

6.1.1 Lightning Arresters

A double overlay (Figure 24) has been made at K-band with and without lightning arresters. The agreement in side lobes, as judged from this figure, indicates little or no effect caused by the arresters.

6.1.2 Side Lobes

6.1.2.1 L-Band (H-Plane)

The free space H-plane pattern is quite asymmetrical (Pattern 110). In horizontal polarization there is a 14-dB side lobe on the bottom which would intersect the ground for the 0° through 70° angles. On the top, the side lobe is 20 dB and is a double lobe. Neither radome changed the bottom side lobe, but both increased the top to 14 dB by breaking up the double lobe.

Side-lobe level changes for the H-plane patterns can be seen from Table 5. On the 90° side there is excellent agreement for all four angles between free space and both radomes. On the 270° side, the radomes do increase the level of the first lobe, again by breaking up the double lobe.

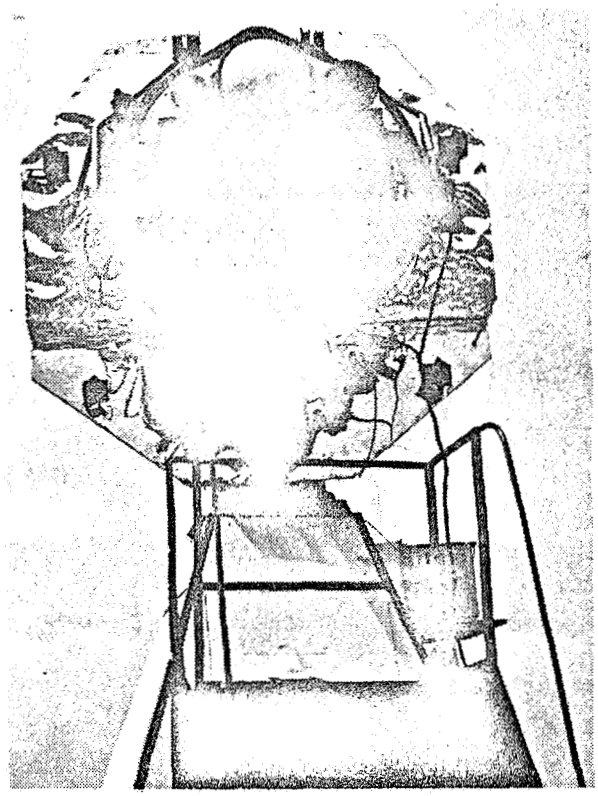

Figure 22. Antenna System, Mount, and Test Pedestal

Comparing the H-plane patterns for free space for the four angles, it can definitely be concluded that the structure does not affect the patterns (see patterns 108, 110, 112, and 114).

The elevation patterns (Table 5) show higher side lobes than those in Table 6. As mentioned above, the vertical plane is skewed and patterns are not taken through the peak of the beam.

6.1.2.2 L-Band (E-Plane)

On the 90° side for horizontal polarization, there is one case of a 2-dB increase in side lobe. In several other cases the side lobes were actually decreased (see Table 6). On the 270° side there were no increases in the first side lobe caused by the radomes.

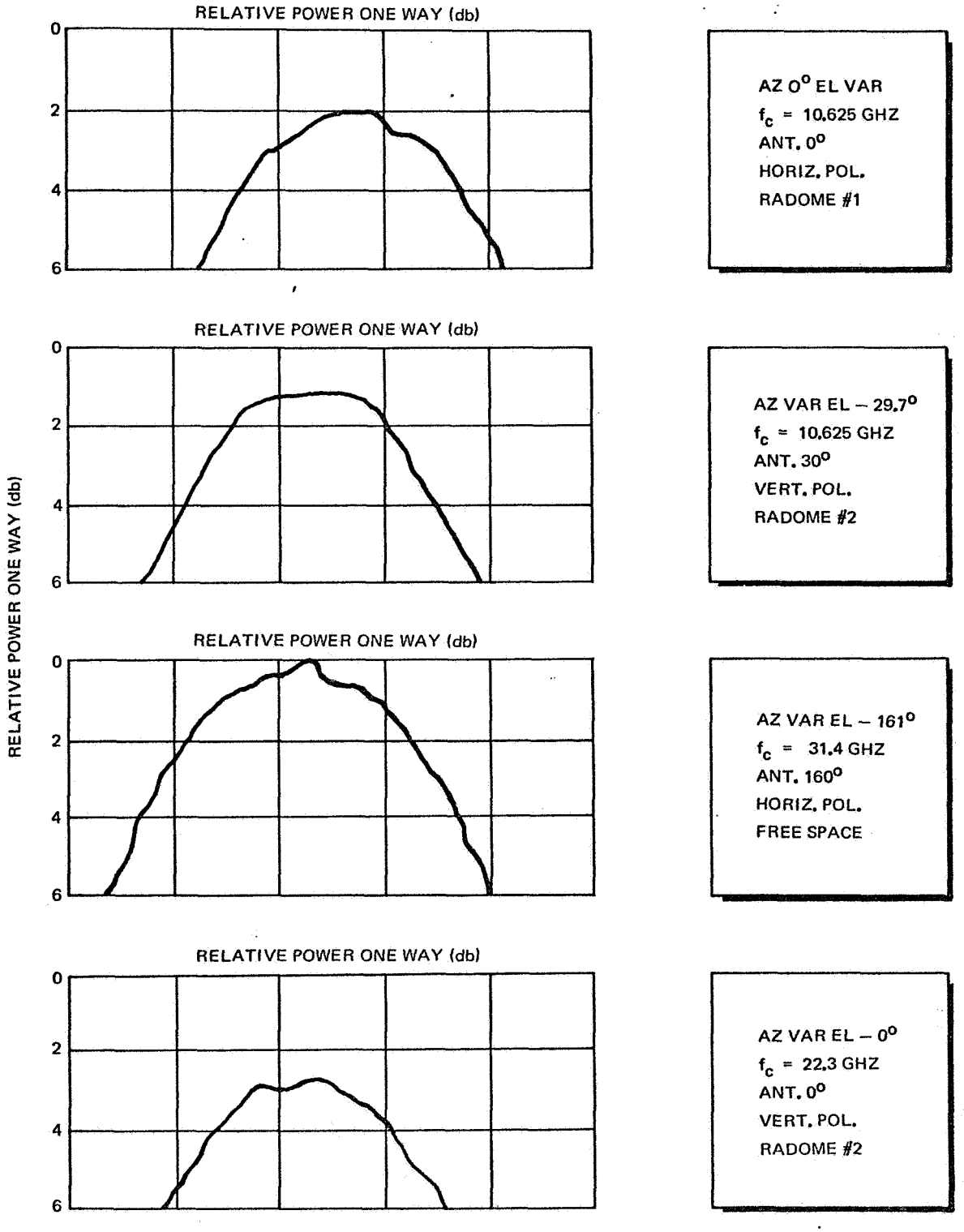

Figure 23. Variation in Main Beam Shape

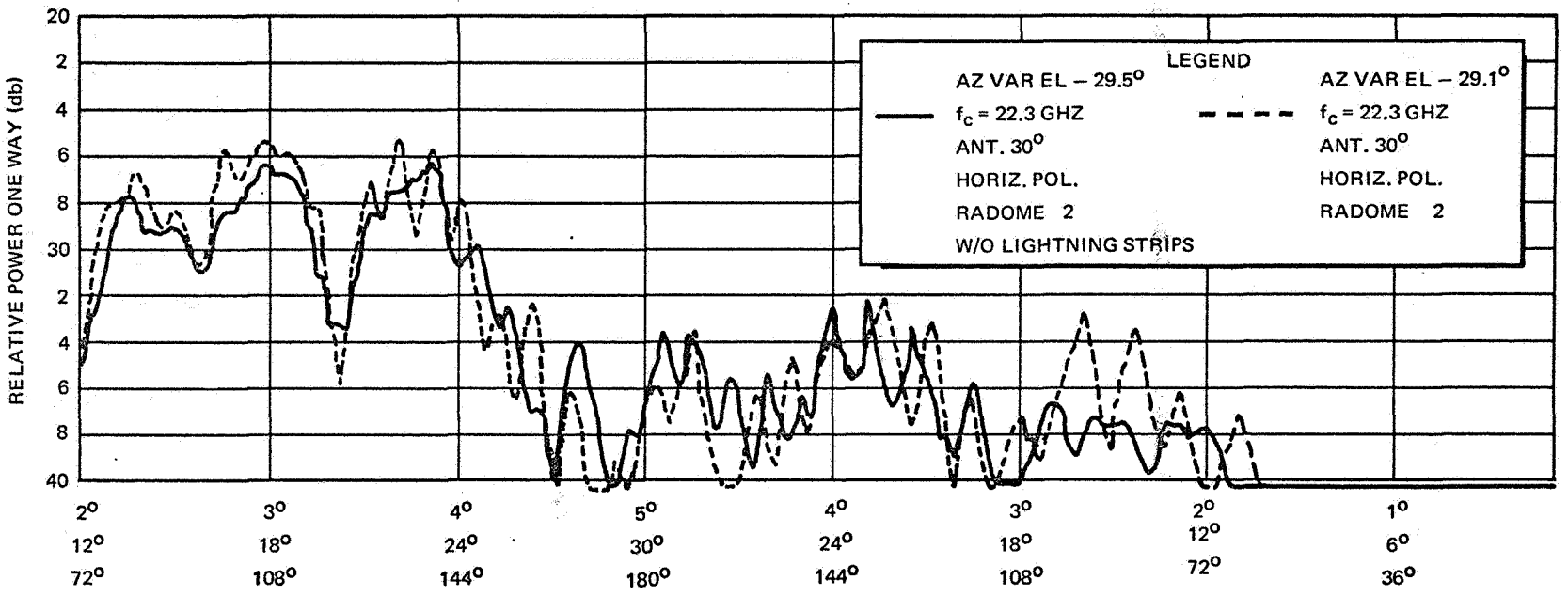

Figure 24. Effect of Lightning Arrester on Side-Lobe Structure

6.1.2.3 X-Band (H-Plane)

For vertical polarization the main beam in each set of patterns (free space, radome 1, and radome 2) was badly notched. At the 160° angle there is a great increase in all the side lobes for both radomes, radome 1 having a 15-dB lobe at 60° from the main beam. At the 30° angle, there is a somewhat small increase in side-lobe energy. The first lobes, however, in all cases except the 160° angle are down less than 3 dB (see Table 11).

For horizontal polarization, the notch still appears and the 160° angle has increased side-lobe energy (see Table 8).

6.1.2.4 X-Band (E-Plane)

There is one first side lobe which changes 3 dB going from free space to the radome. It occurs on the 270° side of radome 1 at the 160° angle (see Pattern 58). All other lobes match within 3 dB, the specification value (see Table 9). The patterns for the 160° angle for both radomes show higher lobes at about 30° off the main beam, because the X-band horn is quite close to the temperature-sensing wires.

Table 10 gives the results of the E-plane taken by elevation patterns. In each of these patterns the main lobe has a notch on it. This occurred on the other polarization also.

6.1.2.5 K-Band (H-Plane)

There is a variation of 2 dB in free-space patterns over the four angles 0°, 30°, 70°, and 160°. However, the first side lobe for the patterns for both radomes are within 3 dB of the free-space value for each corresponding angle except for radome 2 at the 30° angle on the 90° side where the increase is 4 dB (see Pattern 166). There is an increase in side-lobe energy for the 0° angle 36° off the main beam for both radomes and at the 30° angle for radome 2 only. The other angles had no increased energy into the side lobes (see Table 15). Notches and flat tops occur in each set of patterns.

6.1.2.6 K-Band (E-Plane)

The first side-lobe level is within specification for all angles on both radomes (see Table 13), except for the 160° angle on radome 2 where the increase is 4 dB (see Pattern 210). At this angle also there is increased energy in the other side lobes. Notches and flat tops occur in each set of patterns.

It is interesting to note that the corresponding pattern for vertical polarization does not have this increase in side lobe nor the increased energy in the other side lobes (see Pattern 169 and Table 14).

6.1.2.7 K_a-Band (H-Plane)

The vertical polarization patterns for both radomes match the free-space pattern within 3 dB except at the 160° angle. At this angle for both radomes, there is increased energy in the side lobes (see Patterns 154 and 164). The free-space main beam has a notch at all angles and the results seem to be that the patterns with radomes then tend to have a 2 to 3 dB ripple (see Table 19).

6.1.2.8 K_a-Band (E-Plane)

The free space patterns have a notch on them and the patterns with radome have a ripple on them. The side lobes with radome on have good agreement with free space again with the exception of the 160° angle (see Table 17 and Patterns 50 and 218).

6.1.3 Beam Shift

6.1.3.1 L-Band (E-Plane)

There is a 1.3° shift in beam from the 30° angle to the 160° angle for the free-space pattern. Whereas the maximum shift from free space due to the radome is 0.25° for radome 1 at the 160° angle and 0.2° for radome 2 at the 70° angle. The specification is 3° so the effect is quite small (see Table 5).

6.1.3.2 L-Band (H-Plane)

There is a 0.3° shift in beam from the 30° angle to the 160° angle for the free-space pattern. However, the maximum shift from free space due to the radome is 1° for radome 1 at the 160° angle and 1.2° for radome 2 also at the 160° angle (see Table 7).

6.1.3.3 X-Band (E-Plane)

For horizontal polarization, the shift in beam for both radomes was 0.2° or under all angles, except the 160° angle on radome 2 where the shift was 1.15° (see Table 9).

6.1.3.4 X-Band (H-Plane)

For vertical polarization, the beam shift was quite large, the highest being 1.65° for the 160° angle on radome 2. Again these patterns (Table 11) had notches and flat tops occurring even on the free-space beam.

6.1.3.5 K-Band (E-Plane)

The maximum beam shift for the free-space beam over the four angles is 1.05°. However, for the radomes the maximum change from free space occurs at the 0° angle, on radome 2 where the change is 0.8° (see Table 13).

6.1.3.6 K-Band (H-Plane)

The free-space beam over the four angles shows only a 0.25° change (see Table 15). There is a 1.2° change in radome 2 at the 30° angle. Sidelobe energy is high (see Pattern 166).

6.1.3.7 K_a-Band (E-Plane)

The beam shift is less than 0.2° for both radomes except for the 160° angle. Here the shift is 1.75° for radome 1 and 1.05° for radome 2.

6.1.3.8 K_a-Band (H-Plane)

The greatest change for this polarization occurs at the 30° angle where the shift is 1.05°.

6.1.4 Beam Width

6.1.4.1 L-Band (E-Plane)

There is a 0.3° (1.9%) maximum change in beam width for the four angles for the free-space patterns. The greatest change caused by the radome occurs at the 70° angle for radome 1 where the change is 9.4%. Radome 2 has a maximum of 6% at the 30° angle. Specification is 10% (see Table 5).

6.1.4.2 L-Band (H-Plane)

There is a 0.7° (4.7%) maximum change in beam width for the four angles for the free-space patterns. The greatest change caused by the radome occurs at the 0° angle for radome 2 where the change is 5.5%. Radome 1 has a maximum of 4.7% at the 0° angle (see Table 7).

6.1.4.3 X-Band (E-Plane)

The beam width varied no more than 0.15° from the average value. The beam width appears to be virtually unchanged by the radomes. Notches do appear in the main beam (see Table 9).

6.1.4.4 X-Band (H-Plane)

Azimuth patterns taken with vertical polarization generally had a notch on the main beam. This occurred with radomes and free space. Patterns 128, 130 and 96 had a flattened main-beam peak. The beam width in these cases was unaffected in value. The notches and flat top were at the 30° and 70° angles where the array is clear of radome sensor wires. In particular, the flattened free-space pattern (Pattern 96) was at the 70° angle (see Table 11). Elevation patterns with horizontal polarization has some notched main beams, two of which were free space but no flattened tops (see Table 8).

6.1.4.5 K-Band (E-Plane)

Radome 1 and free-space beam widths compare quite well. Radome 2 has a decided increase in beam width, for all four angles giving a maximum increase of 0.8° at the 160° angle. These patterns indicate a general increase in side-lobe level (see Table 13).

6.1.4.6 K-Band (H-Plane)

The beam width is quite constant for both radomes varying only 0.3° for radome 1 at the 0° angle (see Table 15 and Pattern 140).

6.1.4.7 K_a-Band (E-Plane)

There is a difference of 0.4° in the beam width for the free-space patterns going from the 0° angle to the 30° angle. All beams have a notch on them, the 160° angle having a 1/2-dB notch. The beam widths vary from 5.1° to 6.1°.

6.1.4.8 K_a-Band (H-Plane)

The free-space patterns for all four angles have only 0.1° variation in beam width. Both radomes have beam-width values close to free space, except for the 160° angles.

6.2 TRANSMISSION TESTS

When MDAC was requested to use the antenna package supplied by MSC instead of individual antennas, it was understood that the techniques for transmission measurements given in MIL-R-7705A (ASG) 12 January 1955, could not be followed. It would not be possible to move the radome with respect to the antennas the required one-quarter wavelength. The radome, however, could be moved off and on the mockup fixture within 5 min and it was felt that good comparative tests could therefore be made. At each frequency and polarization, the equivalent angle used for the on-off comparison was 0°. Readings were then taken for the other angles (30°, 70°, and 160°) with radome on and compared to the 0° angle reading. It was understood that along with the inability to move the radome one-quarter wavelength that any mismatch in the antenna system would degrade the accuracy of the readings. The readings obtained are presented in Table 22.

It was agreed by the technical personnel from MSC, JPL and MDAC that transmission reading would be taken on the radomes during the calibration tests run by JPL at their Table Mountain facility. The partial results from

Table 22

TRANSMISSION LOSS IN dB

Radome	Frequency (GHz)	Polarization	Angle (deg) 0	20*	30	70	160	Specification
1	31.4	Horizontal	2.1	1.2	2.2	1.5	3.2	1.6
	22.3	Horizontal	1.6	1.0/0.9**	1.2	0.8	1.7	1.1
	10.6	Horizontal	0.5	0.5	0.4	0.6	1.3	0.5
	1.4	Horizontal	1.2	0.2	0.4	0.3	0.6	0.5
	31.4	Vertical	1.8	1.4	1.6	2.0	2.9	1.6
	22.3	Vertical	2.0	1.5/1.4	1.7	0.6	1.5	1.1
	10.6	Vertical	1.2	0.5	0.7	0.4	1.6	0.5
	1.4	Vertical	0.5	0.3	0.6	0.7	0.5	0.5
2	31.4	Horizontal	1.8	1.4	1.3	1.6	2.7	1.6
	22.3	Horizontal	2.5	1.0/1.0	1.8	1.6	2.9	1.1
	10.6	Horizontal	0.6	0.5	0.4	0.5	1.5	0.5
	1.4	Horizontal	1.2	0.4	0.6	0.7	0.6	0.5
	31.4	Vertical		1.4				1.6
	22.3	Vertical		1.6/1.6				1.1
	10.6	Vertical		0.5				0.5
	1.4	Vertical		0.4				0.5

*JPL measurements

**Two frequencies were measured in the K-band region

these measurements on transmission are also given in Table 22 for an averaged value (20° to 70°). These numbers represent the absorptive losses caused by the radome.

Tests were made for a few angles with and without the lightning arresters (in place) along with one test run to determine any effect in transmission due to the presence of the temperature-sensing wires. The final results of these tests will be in a JPL report.

A review of Table 22 gives no conclusive results. Some indication of the ambiguity can be seen if the data are compared as follows:

1. Exclude the MDAC results from angles 0° and 160° because of some of the pattern changes observed at these angles.
2. Exclude K-band temporarily.
3. JPL data show both radomes at or below specification for the three frequencies. MDAC data show each radome equally in and out of specification with no apparent order corresponding to angle, polarization, or radome.
4. Considering now the K-band reading, JPL data show both radomes on horizontal polarization to be in specification while the MDAC data show radome 1 and radome 2 out. Conversely, JPL data show both radomes out at vertical polarization and MDAC (on radome 1) show one angle in and one angle out.